REPORT DOCUMENTATION PAGE	*Form Approved OMB No. 0704-0188*

The public reporting burden for this collection of information is estimated to average 1 hour per response, including the time for reviewing instructions, searching existing data sources, gathering and maintaining the data needed, and completing and reviewing the collection of information. Send comments regarding this burden estimate or any other aspect of this collection of information, including suggestions for reducing the burden, to Department of Defense, Washington Headquarters Services, Directorate for Information Operations and Reports (0704-0188), 1215 Jefferson Davis Highway, Suite 1204, Arlington, VA 22202-4302. Respondents should be aware that notwithstanding any other provision of law, no person shall be subject to any penalty for failing to comply with a collection of information if it does not display a currently valid OMB control number.

PLEASE DO NOT RETURN YOUR FORM TO THE ABOVE ADDRESS.

1. REPORT DATE *(DD-MM-YYYY)*
20/Sep/2001

2. REPORT TYPE
THESIS

3. DATES COVERED *(From - To)*

4. TITLE AND SUBTITLE
VEGETATION IMPACTS ON MAXIMUM AND MINIMUM TEMPERATURES IN NORTHEAST COLORADO

5a. CONTRACT NUMBER

5b. GRANT NUMBER

5c. PROGRAM ELEMENT NUMBER

6. AUTHOR(S)
CAPT HANAMEAN JAMES R JR

5d. PROJECT NUMBER

5e. TASK NUMBER

5f. WORK UNIT NUMBER

7. PERFORMING ORGANIZATION NAME(S) AND ADDRESS(ES)
COLORADO STATE UNIVERSITY

8. PERFORMING ORGANIZATION REPORT NUMBER
CI01-253

9. SPONSORING/MONITORING AGENCY NAME(S) AND ADDRESS(ES)
THE DEPARTMENT OF THE AIR FORCE
AFIT/CIA, BLDG 125
2950 P STREET
WPAFB OH 45433

10. SPONSOR/MONITOR'S ACRONYM(S)

11. SPONSOR/MONITOR'S REPORT NUMBER(S)

12. DISTRIBUTION/AVAILABILITY STATEMENT
Unlimited distribution
In Accordance With AFI 35-205/AFIT Sup 1

13. SUPPLEMENTARY NOTES

14. ABSTRACT

DISTRIBUTION STATEMENT A
Approved for Public Release
Distribution Unlimited

20011016 180

15. SUBJECT TERMS

16. SECURITY CLASSIFICATION OF: a. REPORT	b. ABSTRACT	c. THIS PAGE	17. LIMITATION OF ABSTRACT	18. NUMBER OF PAGES	19a. NAME OF RESPONSIBLE PERSON
				67	19b. TELEPHONE NUMBER *(Include area code)*

THESIS

VEGETATION IMPACTS ON MAXIMUM AND MINIMUM TEMPERATURES IN NORTHEAST COLORADO

Submitted by

James R. Hanamean, Jr.

Department of Atmospheric Science

In partial fulfillment of the requirements

for the degree of Master of Science

Colorado State University

Fort Collins, Colorado

Fall 2001

COLORADO STATE UNIVERSITY

May 15, 2001

WE HEREBY RECOMMEND THAT THE THESIS PREPARED UNDER OUR SUPERVISION BY JAMES R. HANAMEAN, JR. ENTITLED VEGETATION IMPACTS ON MAXIMUM AND MINIMUM TEMPERATURES IN NORTHEAST COLORADO BE ACCEPTED AS FULFILLING IN PART REQUIREMENTS FOR THE DEGREE OF MASTER OF SCIENCE.

Committee on Graduate Work

Committee Member

A. Scott Denning

Committee Member

Roger A. Pielke

Adviser

Department ~~Head~~ acting

ABSTRACT OF THESIS

VEGETATION IMPACTS ON MAXIMUM AND MINIMUM TEMPERATURES IN NORTHEAST COLORADO

The impact of vegetation on the microclimate has not been adequately considered in the analysis of temperature forecasting and modeling. Vegetation has transpirational and evaporational influences in the area it inhabits, affecting the surface energy budget. The presence of vegetation, as compared to bare soil, modulates the diurnal temperature cycle. During the day, transpiring vegetation partitions a greater portion of the incoming solar energy into latent heat, decreasing the maximum temperature. At night, the vegetated area radiates energy and allows condensation, increasing the minimum temperatures via latent heat release.

A daily 850-700 mb layer mean temperature, computed from the National Center for Environmental Prediction-National Center for Atmospheric Research (NCEP-NCAR) reanalysis, and satellite-derived greenness values, as defined by NDVI (Normalized Difference Vegetation Index), were correlated with surface maximum and minimum temperatures at six sites in Northeast Colorado for the years 1989-98. These sites encompass a wide array of environments, from irrigated-urban to short grass prairie. The explained variance ($r-$squared value) of surface maximum and minimum temperature by only the 850-700 mb layer mean temperature was subtracted from the corresponding explained variance by the 850-700 mb layer mean temperature and NDVI values. The subtraction shows that by including NDVI values in the analysis, the $r-$squared values, and thus the degree of explanation of the surface temperatures, increase by a mean of 6 percent for the maxima and 8 percent for the minima over the period March through October. At most sites,

there is a seasonal dependence in the explained variance of the maximum temperatures because of the seasonal cycle of plant growth and senescence. Between individual sites, the highest increase in explained variance occurred at the site with the least amount of anthropogenic influence.

This work suggests the vegetation state needs to be included as a factor in surface temperature forecasting, numerical modeling, and climate change assessments.

James R. Hanamean, Jr.
Department of Atmospheric Science
Colorado State University
Fort Collins, Colorado 80523
Fall 2001

ACKNOWLEDGEMENTS

I would like to thank my adviser, Roger Pielke Sr, for his direction, ideas, and support. Thanks to the members of my committee, Scott Denning and Dennis Ojima, for their support and suggestions. A special thanks to the members of the research group for their assistance: Chris Castro for direction, encouragement, proofreading and clarifying ideas; Glen Liston for aid in programming and concepts; Nolan Doesken for helpful comments and insights; Odie Bliss for her large contributions to locating data; and Dallas Staley for her outstanding administrative support.

This research was supported by the Air Force Institute of Technology and funding for computer support was provided by NSF Grant No. ATM-9910857.

TABLE OF CONTENTS

LIST OF FIGURES

LIST OF TABLES

Chapter 1

INTRODUCTION

1.1 Vegetation and Climate

Climate should be considered from a greater perspective than simply a long-term record of weather observations. The soils, vegetation, terrain, and surface water systems all play an important role in the interaction between the biosphere and the atmosphere. Vegetation effects on the atmosphere are significant, and because they are often so highly correlated, in some cases climate observations alone have been used as a proxy for vegetation cover (Holdridge 1947). Yet many of the specifics of this relationship have yet to be resolved. Assuming that the reflectivity would be the largest impact due to a change in vegetation, many climate models, both early and recent, estimated the impacts of vegetation change simply to be a change in the surface albedo (e.g., Charney et al. 1977; Sagan et al. 1979; Potter et al. 1981; Henderson-Sellers and Gornitz 1984; Meehl 1994; Dirmeyer and Shukla 1994). The albedo acting as the sole vegetational impact dramatically impacted the modeled result and reduced surface temperatures because of a higher reflectance of incoming solar radiation. However, reduced net surface radiation created an associated decrease in precipitation. Evaporation and transpiration decreased on the drier surface, which often overcame the albedo effect and warmed the surface (Chase 1999). Without the consideration of the latent and sensible heat partitioning and the resultant moisture feedback, focusing only on albedo will yield results of landscape change effects which are incomplete.

1.2 Vegetation and Temperature

The impact of surface temperature on vegetation has been studied for years and many concepts and theoretical models have been put forth as a result (Clements 1916; Raschke

1956a,b; Philip 1964; Cowan 1968; Monteith 1975). Everything from transpiration and stomatal resistances to soil moisture and irrigation have been considered and studied. The surface temperature has definite and sometimes quantifiable effects on the vegetation existing in that environment. However, the impact of the vegetation feedback via the partitioning of the latent and sensible heat flux has not been adequately explored. It has been shown that there is a possible mesoscale impact of crop areas that produce a near sea breeze-like circulation in the Midwest (Segal et al. 1989). Likewise, landuse changes over the last century (i.e., urbanization and changes in natural vegetation to cropland) have been modeled, showing a marked difference in the local circulation (Pielke et al. 1999). The partitioning of the latent and sensible heat fluxes near the surface is greatly impacted by the presence or absence of living, transpiring vegetation.

The surface energy budget can be expressed as:

$$R_N = H + H_L + H_G,$$

where R_N is the net radiation, H and H_L are the sensible and latent heat fluxes to or from the air, and H_G is the ground heat flux to or from the submedium (Arya 1988). For this work, the ground heat flux term will be neglected. During the daytime the ground heat flux is small compared to the other fluxes and can be estimated to be zero over vegetated surfaces (Segal et al. 1988). Nighttime ground heat fluxes are larger in proportion to the other fluxes but nearly the same magnitude (though opposite sign) as its daytime counterpart (Arya 1988). With H_G neglected, the resultant equation used as the basis of this work becomes:

$$R_N = H + H_L.$$

The measurements of incoming and outgoing longwave and shortwave radiation can be retrieved from sensor instruments and a net flux calculated. It is clear from this simple equation that the latent heat flux must be considered to arrive at an appropriate and accurate value of the sensible heat flux, and thus the surface temperature. The Bowen ratio, the ratio of the sensible heat flux to the latent heat flux, gives a relational measure of the partitioning of the two fluxes.

This partitioning of the surface heat flux could, if profound enough, impact the depth and character of the atmospheric planetary boundary layer, the winds, the moisture profile, and, of interest here, the surface temperatures. Urban heat island effects are caused not only by the amount of sensible heat from the concrete, metal, and glass of the urban structures and pavements but the lack of latent heat from the absence of broad area vegetation. If planned carefully, vegetation could be used to mitigate some of the anthropogenic effects generated by the development of urban areas (Avissar 1996).

The region of focus in this study is northeast Colorado. This region is characterized by a mix of short grass steppe, urban and rural areas, and croplands. The Platte River Valley provides only a limited natural moisture source for increased humidity in the atmosphere. Of more importance as a moisture source is irrigation. The sites in this study encompass a wide array of environments, from pristine to mixed impact to heavily anthropogenically influenced (see Fig. 1.1).

The purpose of this work is to determine if there is an increase in the explanation of the surface temperature maxima and minima by including vegetation greenness in the analysis.

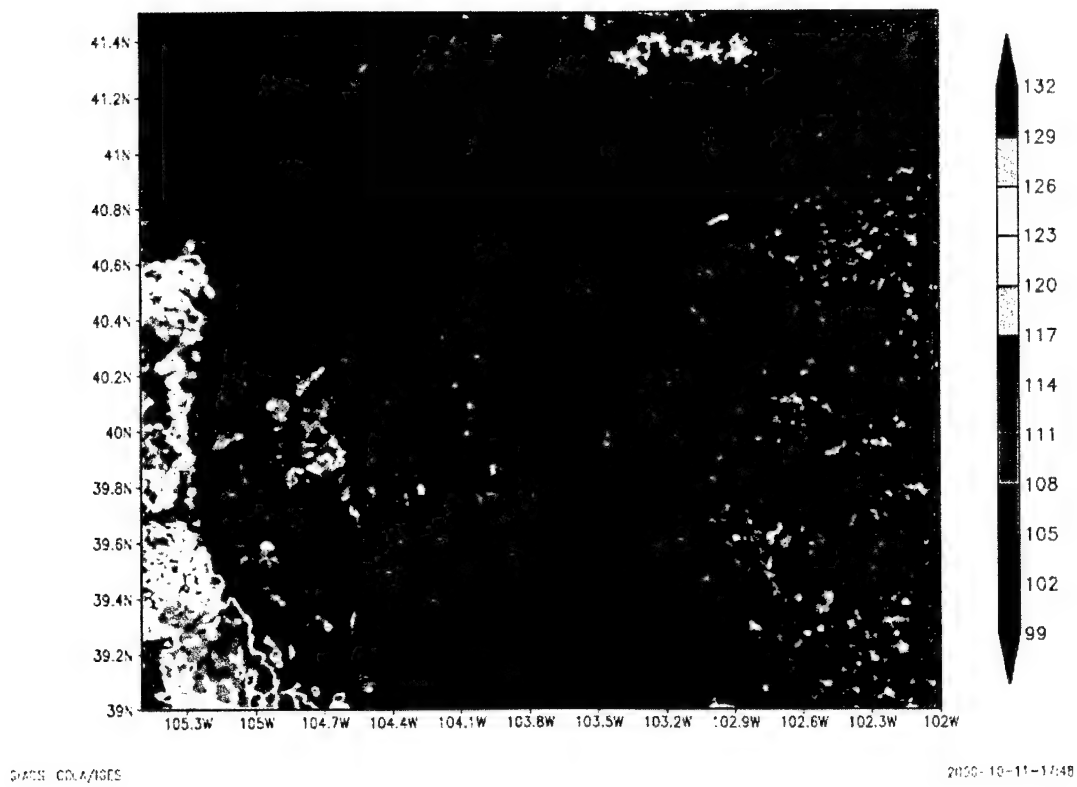

Figure 1.1: Site locations in northeast Colorado.

Chapter 2

SITES

2.1 National Land-Cover Data

A cooperative effort between the U.S. Geological Survey (USGS) and the U.S. Environmental Protection Agency (USEPA) produced a National Land Cover Data (NLCD) set based on 30-meter Landsat thematic mapper data. The predominant land-cover designations of the sites used in this work, as defined by NLCD, are as follows:

a. Grasslands/Herbaceous (71) – areas dominated by upland grasses and forbs. These areas are not subject to intensive management, but they are often utilized for grazing. (Referred to in this work simply as 'grasslands'.)

b. Pasture/Hay (81) – areas of grasses, legumes, or grass-legume mixtures planted for livestock grazing or the production of seed or hay crops. (Referred to in this work simply as 'pasture'.)

c. Row crops (82) – areas used for the production of crops, such as corn, soybeans, vegetables, tobacco, and cotton.

d. Small grains (83) – areas used for the production of graminoid crops such as wheat, barley, oats, and rice.

2.2 Site Designations

Five site designations were created to better classify and explain the varied results from the sites utilized for this work. A Type 1 site is considered pristine, with little or no anthropogenic influences. Type 2 is designated pristine-rural because the sensor is in a location that has some anthropogenic influence though surrounded by pristine-class

landscape. Type 3 is designated rural, where the sensor is strongly influenced by anthropogenic factors though surrounded by pristine to pristine-rural landscape. Conversely, Type 4 is rural-urban, where the sensor location receives a strong vegetational influence though surrounded by urban character landscape. Urban is Type 5. It has almost no vegetational influences and is completely dominated by the urban character. An example of a Type 5 site would be a sensor located on a low roof in downtown Denver. Type 5 cases were not considered in this study. Table 5.1 shows a summary of these designations.

2.3 Surface Metadata

Vegetation and land-surface characteristics of each site examined in this work were detailed first by the NLCD set (see Appendix A). To discern temperature-impacting characteristics in the immediate vicinity, personal inspections of the sites were made. These sites have been used in previous temperature-related studies (Pielke et al. 2000, 2001) and were considered appropriate for this work. Surface data used in this work were collected from the following northeast Colorado sites.

2.3.1 Akron 1N

Akron 1N (40°07′N latitude, 103°10′W longitude) is located at a municipal airport, approximately 8 m from the concrete aircraft apron and runway tarmac to the west (see Fig. 2.1). Thirteen meters to the east is a dirt and gravel parking lot. Metal buildings stand 30 m and 16 m to the north and south, respectively. The landscape surrounding the immediate vicinity is dominated by grasslands in both the 1 km and 5 km radii of examination (see Table A.1 in Appendix A) with a strong residential/commercial presence to the south. Row crops and small grains exist in large swaths in the southeastern two-thirds of the 5 km radius circle around the site (see Fig. A.1). Akron 1N is a Type 2 site.

2.3.2 Akron 4E

Akron 4E (40°09′N latitude, 103°09′W longitude) is located on grassland surrounded by row crops, with a general fallow/row crop mottling throughout the 5-km radius circle

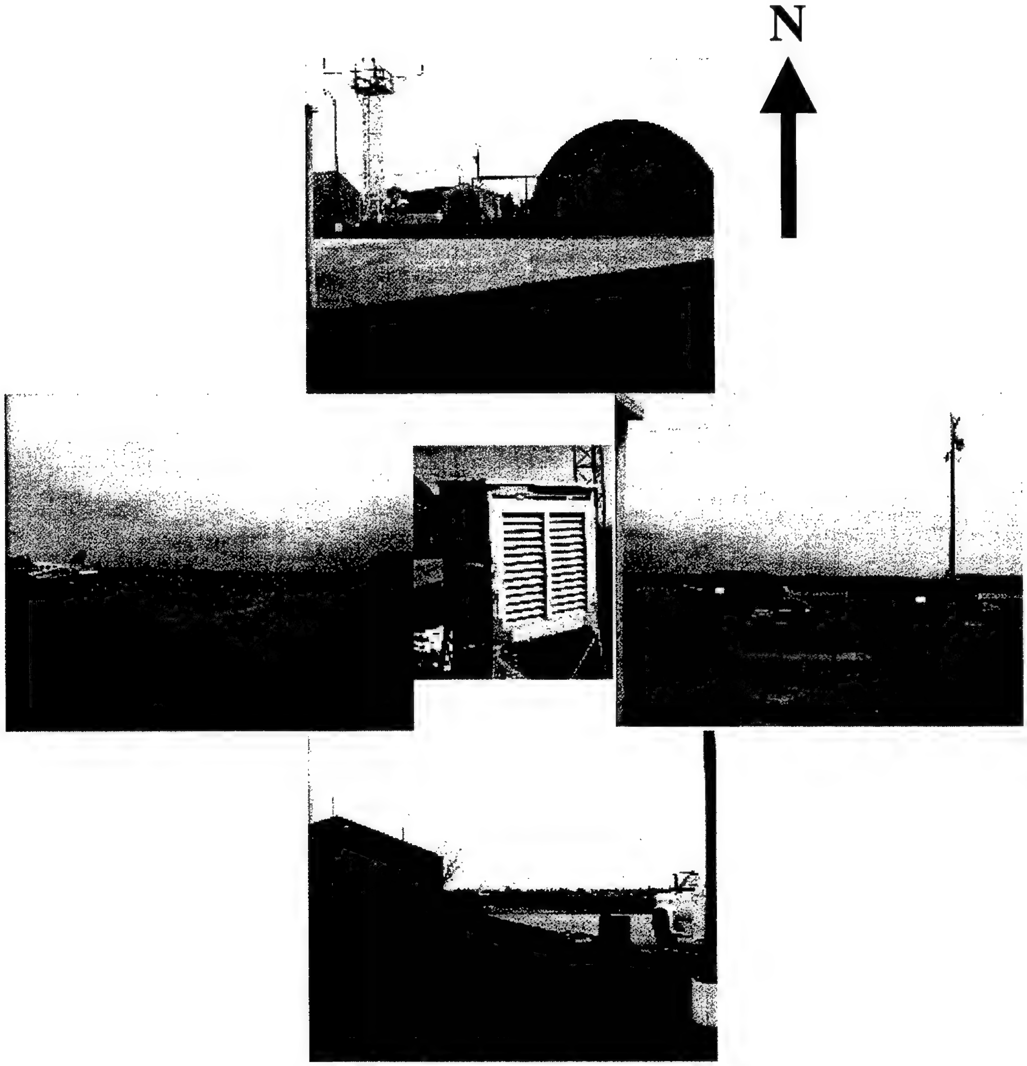

Figure 2.1: Akron 1N site, showing images of the cardinal directions from the sensor.

around the site (see Fig. A.2). Immediately surrounding the site (within 16 m) are irrigated corn and wheat fields. A single line of trees stand less than 1 km to the east (see Fig. 2.2). Akron 4E is a Type 2 site, considered so because of the anthropogenic influence (large-scale irrigation) in the immediate vicinity.

2.3.3 Central Plains Experimental Range (CPER)

The 5-km radius circle around the site location (40°48′N latitude, 104°45′W longitude), is dominated by grasslands. Some small grain areas exist to the south and west. Of the sites examined, this one is considered the most natural or pristine and would probably have the highest vegetational impact (see Figs. 2.3 and A.3). CPER is a Type 1 site.

2.3.4 Fort Collins

The Fort Collins site (40°35′N latitude, 105°05′W longitude) is on the campus of Colorado State University and is immediately surrounded by short grass, a few trees and bushes, and a very large blacktop parking lot (see Fig. 2.4). As a result of the trees and local urban character of the surrounding area, there is less wind at the Fort Collins site. Evaporation rates for this site reflect this lack of wind relative to the other sites. Large-scale irrigation, in the form of lawn maintenance, characterizes the local landscape surrounding Fort Collins and adds a great deal of low-level moisture as well as enhanced greenness even through the more vegetation-stressing periods of July and August (see Fig. A.4). Fort Collins is a Type 4 site.

2.3.5 Fort Morgan

This site (40°16′N latitude, 103°48′W longitude), is surrounded by a mix of residential and commercial influences, grasslands, and row crops. The row crops and grasslands are dominant throughout the 5 km radius circle with the exception of the area to the site's immediate south where residential and commercial influences dominate (see Fig. A.5). The Platte River runs east-west approximately 1 km north of the site. However, the temperature sensor is located 3 m away from a large south-facing brick building, which is part of a much larger factory complex running east-west several hundred meters to either

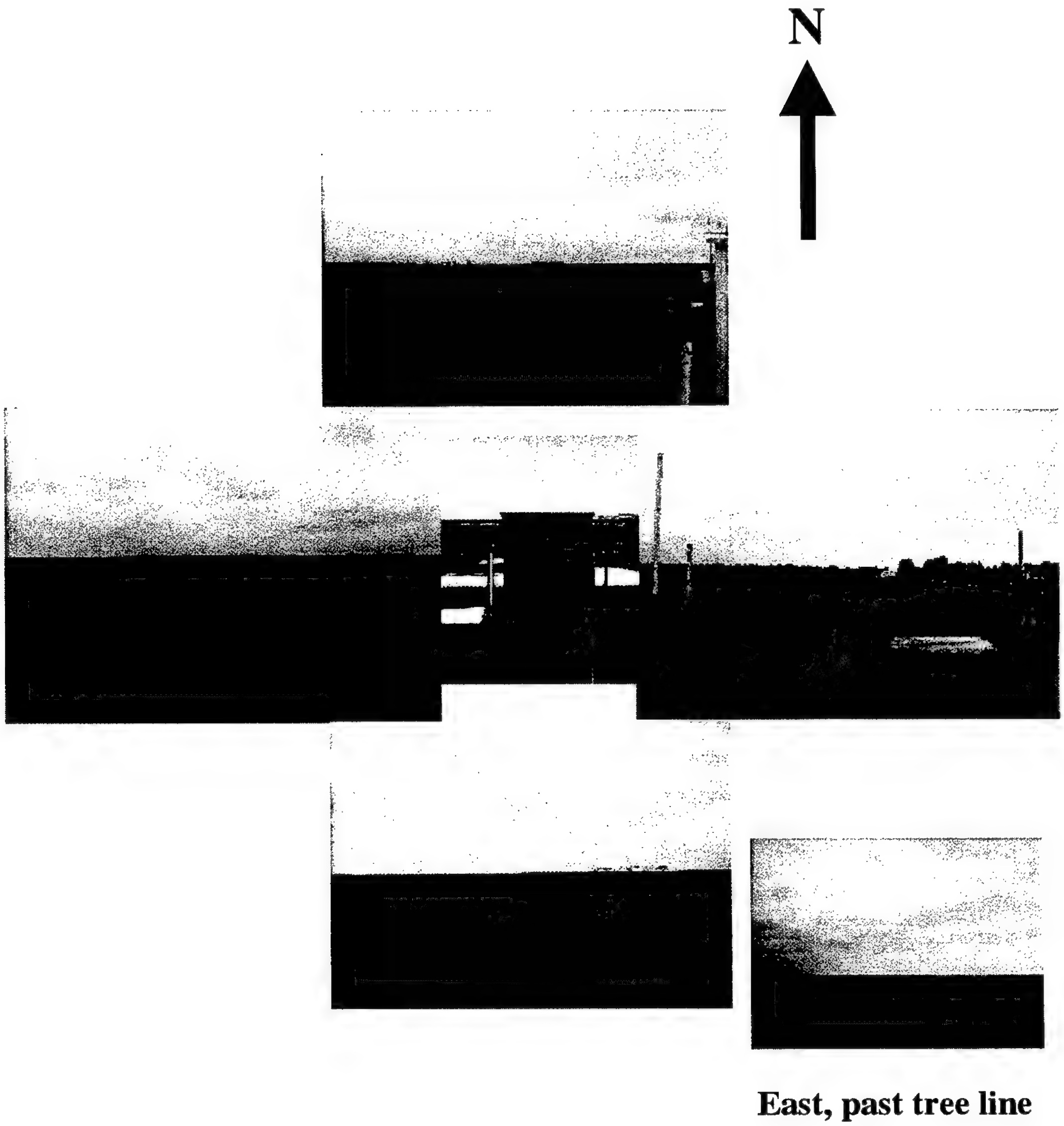

Figure 2.2: Akron 4E site, showing images of the cardinal directions from the sensor.

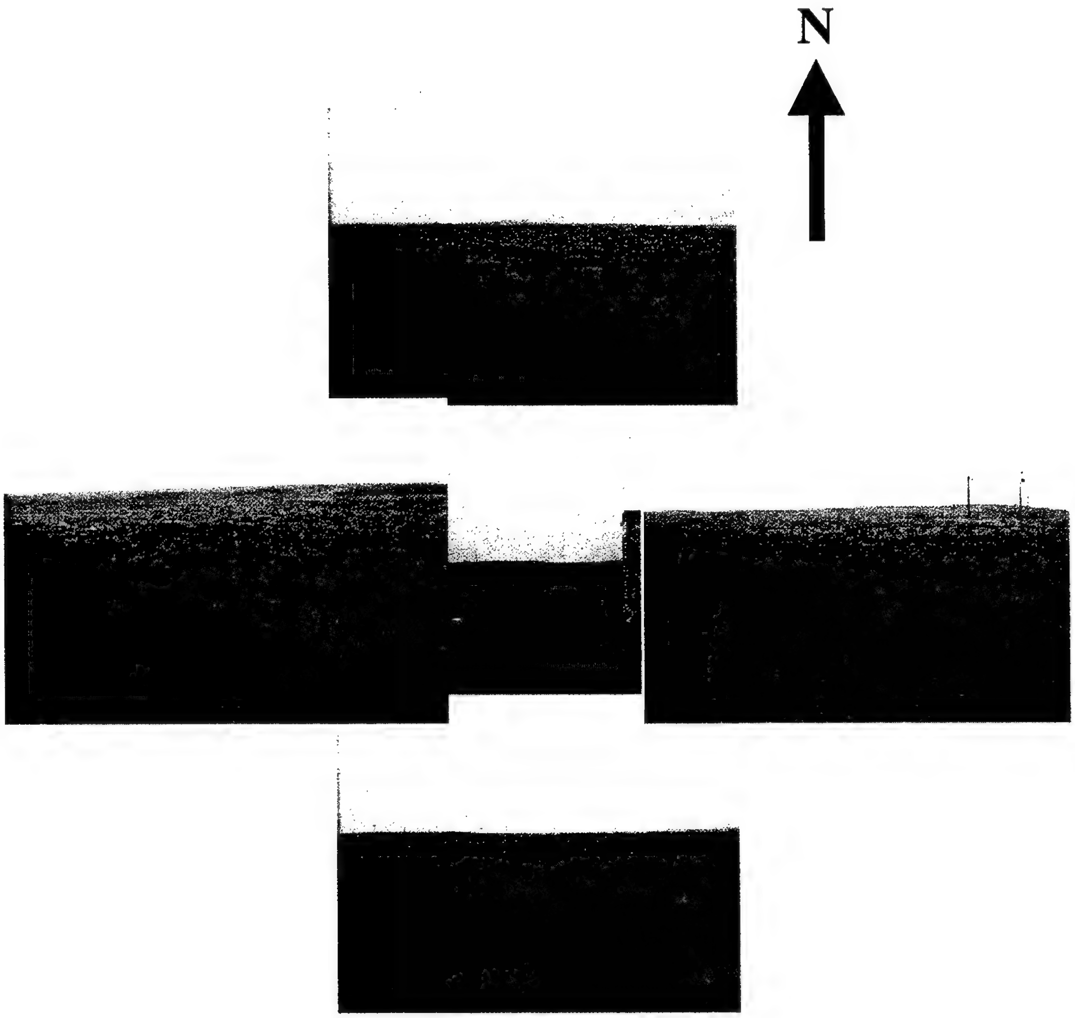

Figure 2.3: CPER site, showing images of the cardinal directions from the sensor.

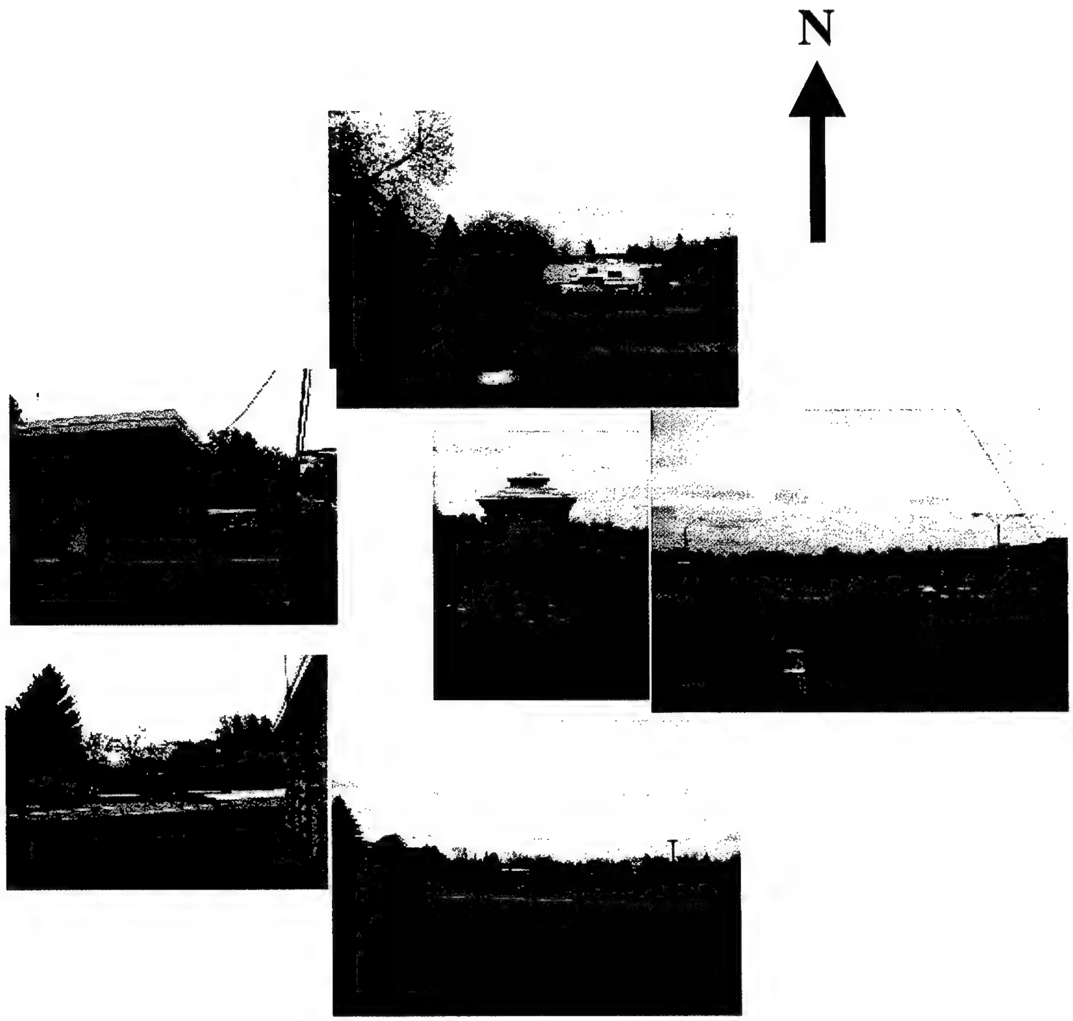

Figure 2.4: Fort Collins site, showing images of the cardinal directions from the sensor.

side (see Fig. 2.5). The factory, which completely shields any northerly influence, has structures made of concrete and metal ranging from 3 to 7 stories. Two and one-half meters behind the temperature sensor is the exhaust of a window air conditioner. To the immediate south of the sensor is a dirt and gravel driveway. A small patch of grassy area extends from the gravel driveway out approximately 70 m but there is a 4500 square meter dirt and gravel parking lot to its immediate west. Fort Morgan is a Type 3 site.

2.3.6 Wray

The Wray site (40°04′N latitude, 102°13′W longitude) is dominated by grasslands with small grains and fallow to the south and southeast, and north (see Fig. A.6). A residential/commercial area is due west – the city of Wray. The sensor is located 1 m from an aluminum-sided single story building, and 3/4 m from a large air conditioning unit/evaporative cooling unit (see Fig. 2.6). The sensor is on the south side of the building approximately halfway down a south-to-north-running slope. To the immediate west is a 10 m valley that could act as a drainage for cooler air. The terrain immediately surrounding the site is hilly with higher elevations to the south. Wray is a Type 3 site.

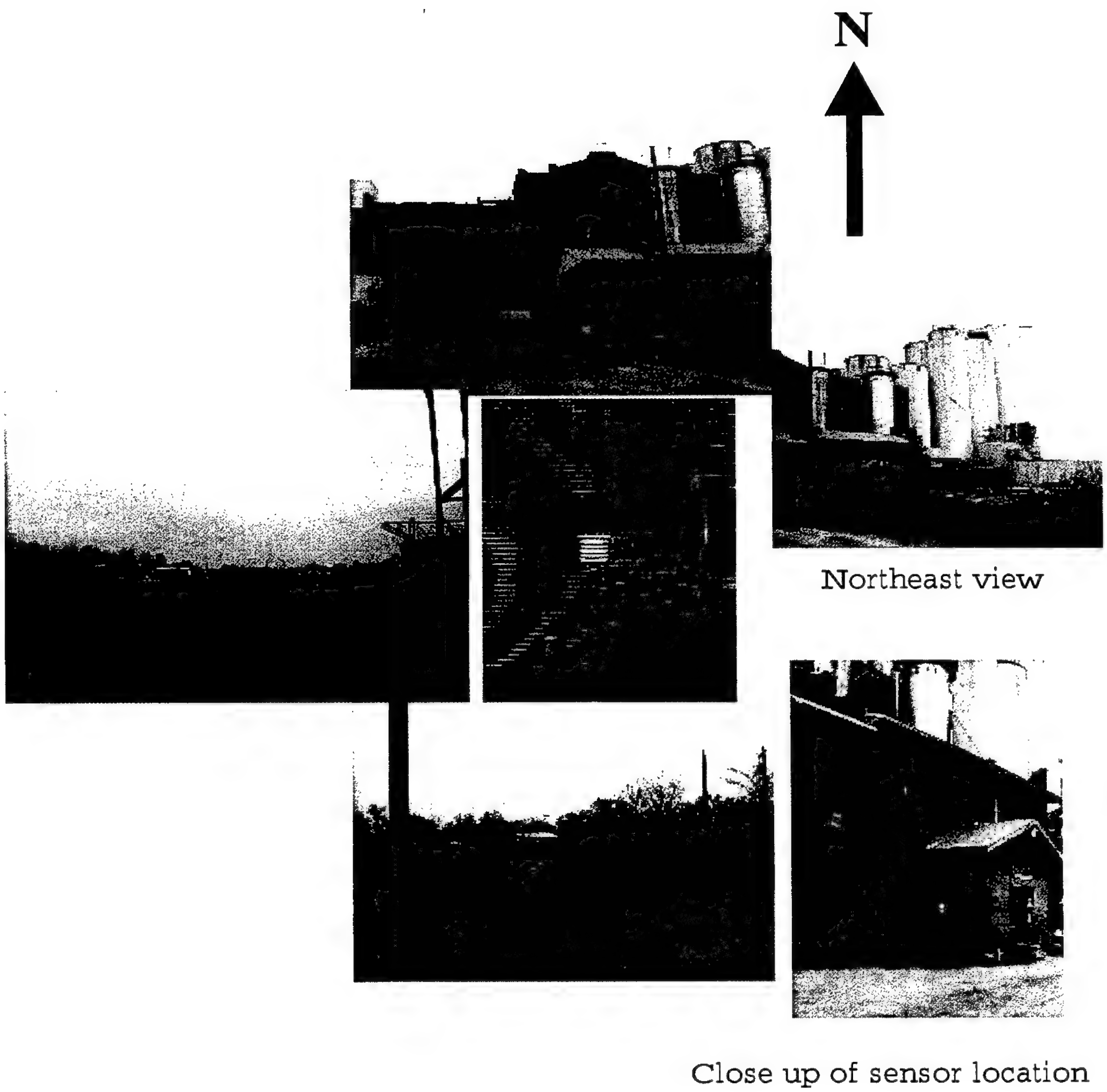

Figure 2.5: Fort Morgan site, showing images of the cardinal directions from the sensor.

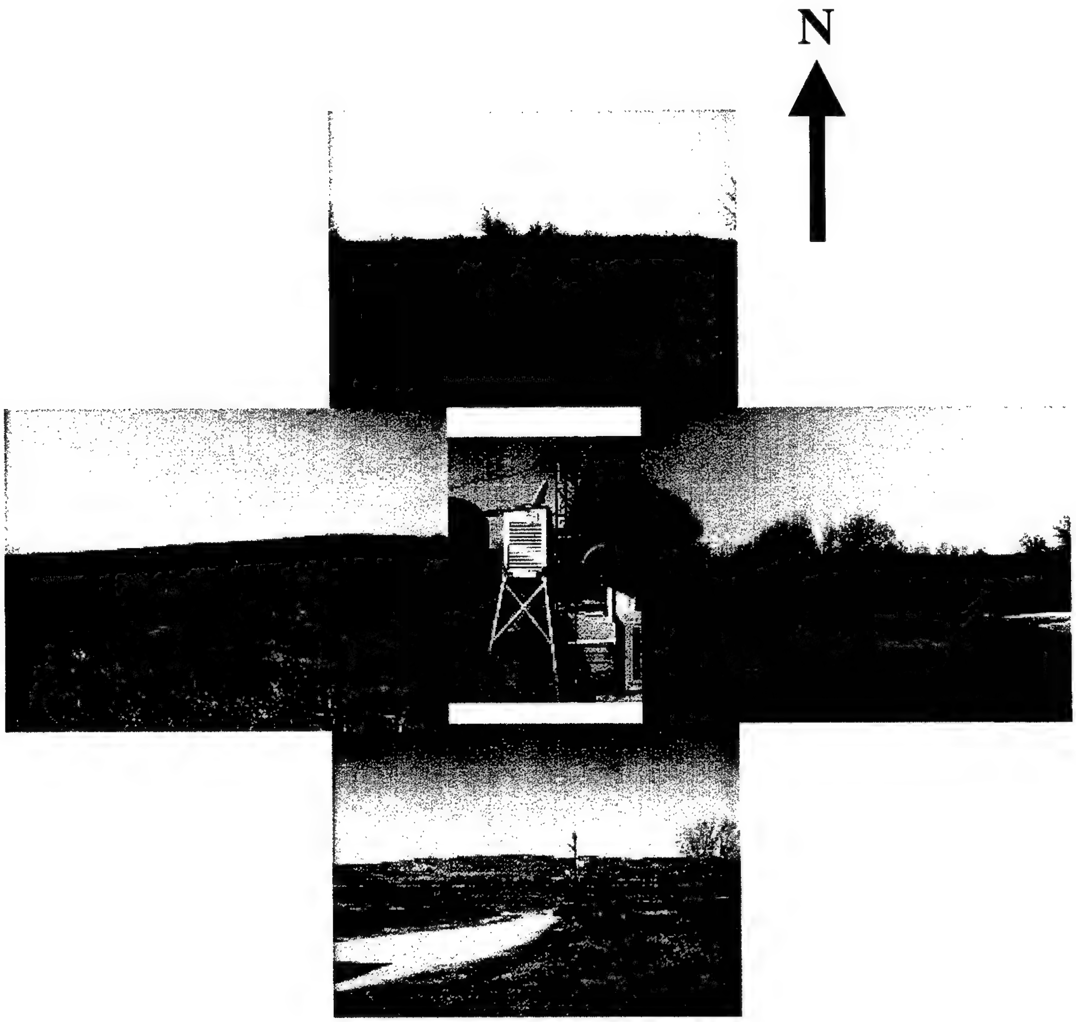

Figure 2.6: Wray site, showing images of the cardinal directions from the sensor.

Chapter 3

DATA

3.1 Upper Air Data

National Centers for Environmental Prediction (NCEP)-National Center of Atmospheric Research (NCAR) reanalysis data at a 2.5° × 2.5° grid spacing were used for the 850 mb and 700 mb temperatures. The data were area averaged for a grid of 5 × 5 degrees (37°–42°N, 105°–100°W). The months of March through October for the years 1989 through 1998 were extracted and used for this work. Reanalysis data were chosen over radiosonde data because of the spatial averaging over northeast Colorado that was required for the analysis. Radiosonde data were only available for two locations, neither of which were representative of the sites under study. The radiosonde data were deemed too location-specific to be utilized for broader area averaging required in this work. Further, the reanalysis lent itself to the area averaging and gave more representative values of the 850 mb and 700 mb temperatures over the sites under study. Reanalysis data has been used for many studies, especially in the continental United States, and is considered reliable. As seen in Fig. 3.1, the 0 Z temperature values are consistently the highest of the four times (0, 6, 12, 18 Z) at the 850 mb level, indicating the general maximum temperature time. Likewise, the 12 Z temperature values are consistently the lowest of the measurements taken at the four times. At the 700 mb level, there is very little variance between the temperatures taken at the four time periods (Fig. 3.2). The 850-700 mb layer mean temperatures mirror the 850 mb results with 0 Z being the time of the temperature maximum and 12 Z being the time of the temperature minimum (Fig. 3.3). Each 0 Z temperature actually occurred during the evening previous, at 18 local time (local for northeast Colorado is Zulu minus 6 hours). The maximum temperatures were

appropriately shifted in the data set. The 850-700 mb layer mean maximum and minimum temperatures were calculated for each day from March through October for the years 1989 to 1998. The layer means were calculated with a simple linear averaging of the 850 mb and 700 mb temperatures.

3.2 Surface Data

3.2.1 Surface Temperatures

The surface temperatures were extracted from the Colorado Climate Center database and the CPER database, based on daily observational measurements. Four sites, Akron 4E, CPER, Fort Morgan, and Wray, took their observations at 0700. The maximum temperature recordings were therefore from the day previous. The maximum surface temperatures were appropriately shifted in the data set. The minimums were not altered. The remaining two sites, Akron 1N, and Fort Collins, took their observations in the evening. The maximum and minimum temperatures recorded were for that day. Thus, no adjustments were required to the data sets for these sites. All temperatures were converted to Kelvin to eliminate the possible difficulties in dealing with positive and negative temperature values in the calculations.

3.2.2 Precipitation

Precipitation data for all sites except CPER were retrieved from the Colorado Climate Center website. CPER data were retrieved from the Natural Resource Ecology Laboratory (NREL) website under the SLIK-ECO download page. (SLIK-ECO is a project combining a collection of models, the Soil Water Model, the Ecotone Model, and the Century Model). CPER precipitation data had to be converted from its metric (centimeter) values to the equivalent English units (one-hundredth of an inch) to be in congruence with the other precipitation measurements. For all sites, missing precipitation measurements were given a value of zero for that day.

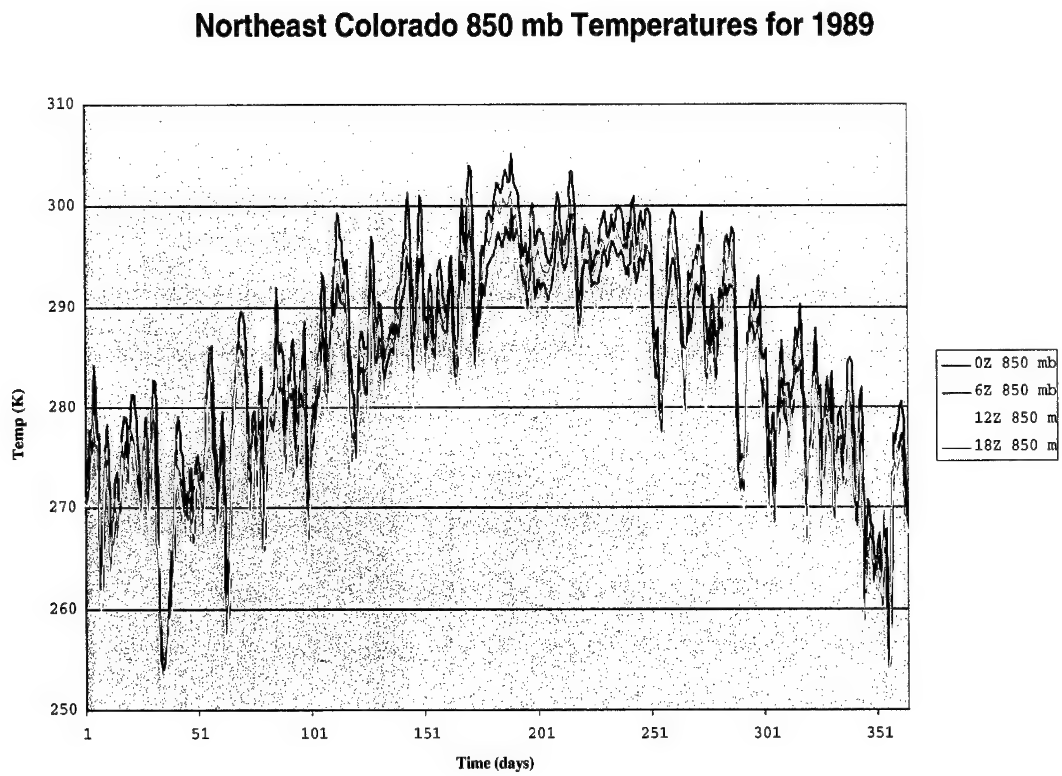

Figure 3.1: Northeast Colorado 850 mb temperatures at 0 Z 6 Z, 12 Z, and 18 Z, showing 0 Z as the time of consistent maximum temperature and 12 Z as the time of consistent minimum temperature.

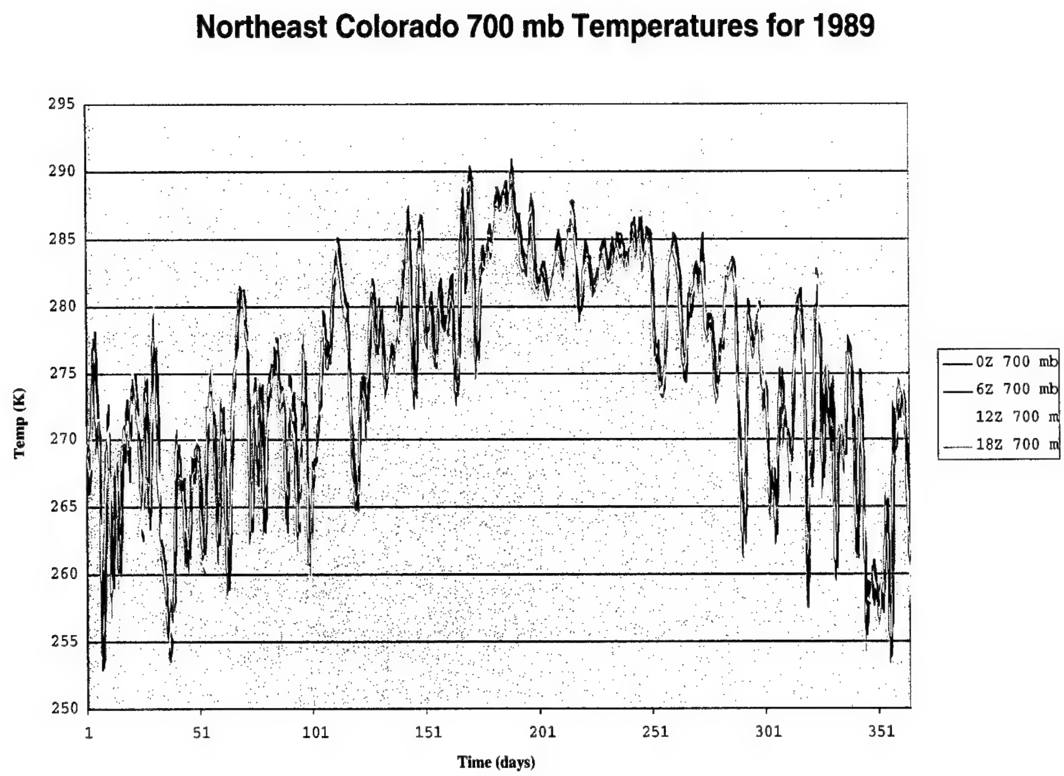

Figure 3.2: Northeast Colorado 700 mb temperatures at 0 Z, 6 Z, 12 Z, 18 Z, showing little variation between any of the measurement times.

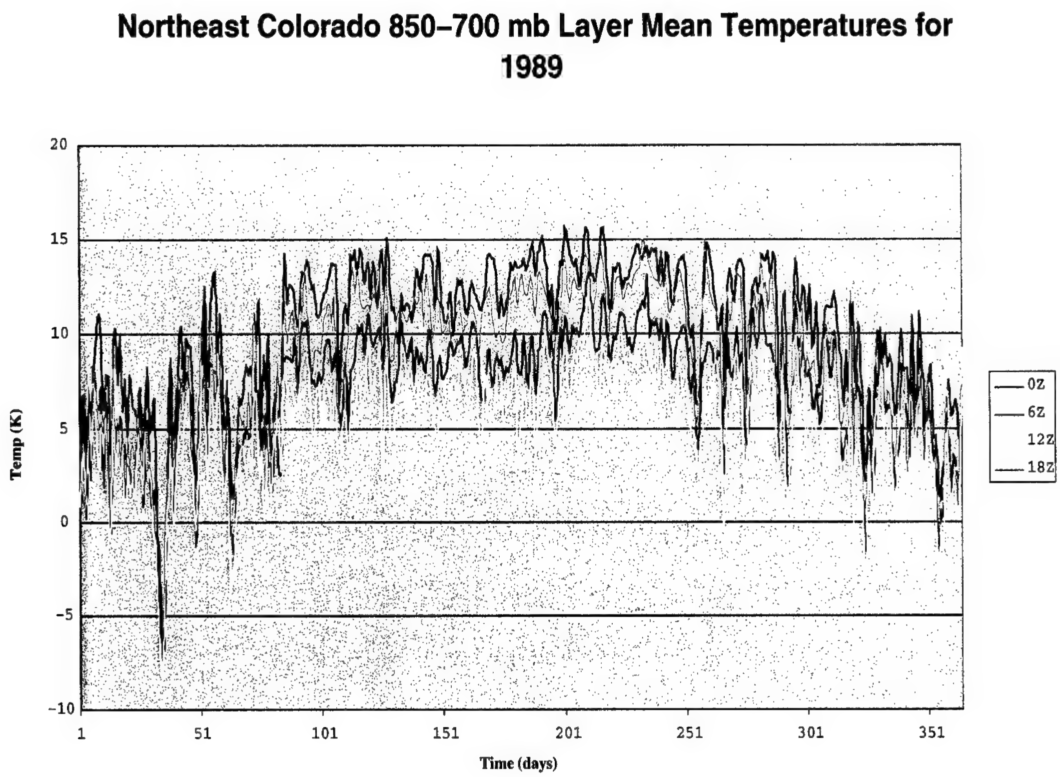

Figure 3.3: Northeast Colorado 850-700 mb layer mean temperatures at 0 Z 6 Z, 12 Z, and 18 Z, showing 0 Z as the time of consistent maximum temperature and 12 Z as the time of consistent minimum temperature.

3.2.3 Evaporation Rates

The evaporation rates were culled from the National Oceanic and Atmospheric Administration (NOAA) Technical Report NWS 34 (Farnsworth and Thompson 1982) and from the Colorado Climate Center. The monthly climatological evaporation rate average for each month, using pan evaporation data, was divided by the number of days in that month to arrive at an estimated daily evaporation value. Akron 1N, Fort Morgan, CPER, and Wray did not have on-site pan evaporation measurements. Pan evaporation measurements from other sites were used for the values of these four sites, taking into account geographic proximity and site similarity. Akron 1N and Akron 4E both used Akron 4E evaporation data. Fort Morgan and CPER utilized the evaporation data from the Wiggins site. Wray was assigned values averaged between Akron 4E and Bonny Dam. Fort Collins had its own evaporation data and was used for that site. The John Martin Dam site was similar to both Akron 4E and Bonny Dam. The March evaporation rates at John Martin Dam were used for the missing March data at all sites utilizing Akron 4E and Bonny Dam data. Because of the general similarities of the rainfall patterns and the site locations between Wiggins and John Martin Dam, Fort Collins and CPER (which utilized Wiggins data) likewise took John Martin Dam March evaporation values for their missing March values.

3.3 Normalized Difference Vegetation Index (NDVI)

3.3.1 General

NDVI is derived from data collected by the Advanced Very High Resolution Radiometer (AVHRR) sensor on NOAA satellites. Digital counts received by channels 1 and 2 of the AVHRR sensor are converted into radiances, normalized for the solar flux at the top-of-the-atmosphere in the bands of 0.5-0.7 microns and 0.7-1.3 microns respectively. Channel 1, which measures radiance values in the visible spectrum, and channel 2, which measures radiance values in the near-infrared, of the sensor are ingested and the NDVI is calculated as follows: NDVI = (NIR - VIS) / (NIR + VIS). VIS and NIR refer to the normalized radiance values of the visible spectrum in channel 1 and the near-infrared in

channel 2, respectively. The magnitude of NDVI is indicative of how much vegetation there is and how well it is doing, from the aspect of photosynthetic activity. The pixel size of the data is 1 × 1 kilometers. The NDVI data were acquired from Dr. Brad Reed at the EROS Data Center. The NDVI measurements were taken every 14 days and indicate the maximum NDVI value during that two week period. NDVI values were extracted for the six sites of interest, using the site latitude and longitude as the center of the NDVI pixel. Where the site was not in the exact center of a data pixel, the pixel center nearest the exact latitude/longitude of the site was automatically extracted. A simple weighting scheme was used to interpolate values for the 13 days between measurements to give a comparative daily value. The weighting scheme is as follows:

$$[\mathrm{NDVI1} * ((15 - \mathrm{day})/14)] + [\mathrm{NDVI2} * ((\mathrm{day} - 1)/14)]$$

where NDVI1 and NDVI2 are two sequential 14-day NDVI values, "day" is the number of the days between the two measurements (the day of a measurement is "day" = 1, the day before a measurement is "day" = 14). Thus, the calculated value at day = 1 is the value of the measurement and has no weight from the next measurement value. The normal values of NDVI, which are –1 to 1, have been scaled to eliminate negative numbers and make them more manageable to compare to other values. The following is the transformation equation:

$$[(\mathrm{NDVI} * 100) + 100] = \text{Scaled NDVI Value}$$

The scaled NDVI values range from 0 to 200.

3.3.2 Sensor Considerations

Though specific impacts are not addressed in this work, several conditions must be noted when using long-term remote sensing data.

The orbital path of the sensor platform can degrade or undergo perturbations which may result in a drifting of the pixelated image or the grid on which it is projected. Pixel drift can also occur as a result of sensor deviations from calibrated standards. Sensor deviation or degradation from calibration tolerances can report incorrect radiance values

that are subsequently converted into incorrect NDVI values. As the sensor degrades over time, the reported greenness values over that time span may follow a reducing trend. When a new and calibrated sensor is placed in operation, the greenness values can suddenly return to greater levels, giving the impression of a sudden greening-up of the landscape.

Cloud cover can have a major impact on surface remote sensing. The high reflectivity of the cloud tops can skew the radiance values to a degree that severely skews or obliterates meaningful NDVI values. To help mitigate this effect, the values reported were from a 14-day period, taking the maximum NDVI value during that period as the actual NDVI value (i.e., with minimized mitigating influences). Soil reflectance can also impact the NDVI values over certain cites, like CPER which has approximately 50% vegetation coverage. The bare soil reflection can skew the NDVI toward lesser values. As well, other atmospheric or site conditions may impact the accuracy of the remote sensing device.

Chapter 4

METHODOLOGY

4.1 Data Format

Data were collected from various sources in various formats. Thirty-meter land use data and the NDVI data were converted and stored in ASCII format for use in the Unix-based Grid Analysis and Display System (GrADS). The upper air temperatures were converted to text files and imported into spreadsheets. The surface temperatures, precipitation measurements, and evaporation data were collected from the different sources and imported or inputted into spreadsheet format. All spreadsheet-formatted data sets were collected and formatted for use in Microsoft Excel spreadsheets and some were further formatted for importing into MathSoft's S-Plus 2000 statistical software package.

4.2 Statistics

Several basic statistical concepts and operations were used for this work. An explanation of terms and their use and implications are detailed in Appendix B.

4.2.1 Coefficient of Determination

The coefficient of determination, or $r-$squared value, is the ratio of the explained variance between two sets of measurement values. Multiplied by 100, the coefficient of determination becomes a percent-explained variance, indicating what percent of the change in one variable is predicted or explained by the change in another. For this work, the $r-$squared value, herein referred to as the explained variance, indicates the degree of explanation of the surface temperature maxima and minima by the 850-700 mb layer mean temperature maxima and minima with and without the inclusion of vegetation impacts via NDVI values. Subtracting the $r-$squared value without the inclusion of vegetational

impacts from the value including those impacts results in an $r-$squared difference value. This difference value will show the change in explanation of the surface temperature extrema by inclusion of the vegetational influences. Typical values for these variables are shown in Table 4.1.

4.3 S-Plus 2000

The statistical software program S-Plus 2000 by MathSoft© was utilized to produce the multiple linear regressions for the analysis. The particular regression utility used was the Robust LTS (Least Trimmed Squares) method. According to S-Plus 4 Guide to Statistics (1997) the Robust LTS regression is a highly robust method for fitting a linear regression model. The LTS estimate β_{LTS} minimizes the sum of the q smallest squared residuals

$$\sum_{i=1}^{q} r_{(i)}^2(\beta)$$

where $r_{(i)}(\beta)$ is the ith order residual. The value of q is often set to be slightly larger than half of n. By contrast, the ordinary least squares estimate β_{LS} minimizes the sum of all of the squared residuals.

$$\sum_{i=1}^{n} r_{(i)}^2(\beta)$$

Robust regression complements classical least-squares techniques where the distribution errors do not satisfy normality conditions (i.e., the errors do not fit a normal distribution) or when the data contain significant outliers. However, the robust regression results are very similar to classical least-squares regressions for normal error distributions. The data sets utilized were assumed to have non-normal error distributions.

4.4 Precipitation Removal

Precipitation events impact the temperature schemes, dramatically reducing the maximum and raising minimum surface temperatures at nearly every occurrence. Figure 4.1 shows the impact of all precipitation events that resulted in more than a trace amount over the period of one year. To better isolate the impacts of the vegetation, the precipitation event days were removed from the analyzed data sets. Precipitation events that

Table 4.1: A data table used in this work, showing the range of $r-$squared values for that site. The values in this table are, in general, indicative of the other sites studied. S stands for surface temperature, L for layer temperature (850-700 mb layer mean temperature), and N for NDVI. The SLN column, therefore, stands for the correlation (squared) between the surface temperature and the layer temperature with NDVI. The SL column is the same, except without the NDVI.

		MAX		**MIN**			**MAX**	**MIN**
		SLN	**SL**	**SN**	**SLN**		**SLN-SL**	**SLN-SL**
89	MA	0.3797	0.3803	0.8216	0.7784	89MA	−0.0006	0.0432
	MJ	0.251	0.2524	0.801	0.7483	89MJ	-0.0014	0.0527
	JA	0.4681	0.4538	0.6783	0.6571	89JA	0.0143	0.0212
	SO	0.6376	0.6159	0.853	0.7917	89SO	0.0217	0.0613
90	MA	0.5406	0.475	0.8189	0.786	90MA	0.656	0.0329
	MJ	0.5799	0.5536	0.8607	0.8597	90MJ	0.0263	0.001
	JA	0.5763	0.5416	0.4251	0.3276	90JA	0.0347	0.0975
	SO	0.4895	0.3793	0.8954	0.8489	90SO	0.1102	0.0465
91	MA	0.07821	0.05076	0.6995	0.6581	91MA	0.02745	0.0414
	MJ	0.7125	0.6397	0.6909	0.6892	91MJ	0.0728	0.0017
	JA	0.4621	0.4419	0.5581	0.4286	91JA	0.0202	0.1295
	SO	0.3953	0.3929	0.8334	0.7036	91SO	0.0024	0.1298
92	MA	0.4604	0.4577	0.5688	0.5163	92MA	0.0027	0.0525
	MJ	0.5172	0.4999	0.6559	0.6539	92MJ	0.0173	0.002
	JA	0.25	0.2552	0.774	0.6947	92JA	-0.0052	0.0793
	SO	0.3696	0.3366	0.7803	0.7711	92SO	0.033	0.0092
93	MA	0.4226	0.3188	0.7522	0.6758	93MA	0.1038	0.0764
	MJ	0.5558	0.5553	0.8796	0.8672	93MJ	0.0005	0.0124
	JA	0.2013	0.1471	0.5942	0.573	93JA	0.0542	0.0212
	SO	0.2361	0.1783	0.7675	0.7662	93SO	0.0578	0.0013
94	MA	0.256	0.2263	0.8216	0.7799	94MA	0.0297	0.0417
	MJ	0.6291	0.6301	0.694	0.6797	94MJ	−0.001	0.0143
	JA	0.3314	0.2394	0.2111	0.2116	94JA	0.092	−0.0005
	SO	0.7772	0.7602	0.9034	0.8873	94SO	0.017	0.0161
95	MA	0.3364	0.3336	0.7141	0.6829	95MA	0.0028	0.0312
	MJ	0.761	0.6656	0.869	0.8116	95MJ	0.0954	0.0574
	JA	0.4341	0.4162	0.6151	0.5909	95JA	0.0179	0.0242
	SO	0.5251	0.4122	0.8522	0.7795	95SO	0.1129	0.0727
96	MA	0.2876	0.2742	0.7904	0.7754	96MA	0.0134	0.015
	MJ	0.4767	0.4606	0.8123	0.7566	96MJ	0.0161	0.0557
	JA	0.5169	0.3079	0.2788	0.2115	96JA	0.209	0.0673
	SO	0.4921	0.4556	0.8393	0.7576	96SO	0.0365	0.0817
97	MA	0.217	0.2026	0.7994	0.7339	97MA	0.0144	0.0655
	MJ	0.4954	0.4958	0.8455	0.8453	97MJ	−0.0004	0.0002
	JA	0.2259	0.2152	0.6209	0.576	97JA	0.0107	0.0449
	SO	0.6238	0.5194	0.7284	0.6618	97SO	0.1044	0.0666
98	MA	0.5559	0.5379	0.6216	0.6183	98MA	0.018	0.0033
	MJ	0.369	0.3587	0.6459	0.6445	98MJ	0.0103	0.0014
	JA	0.631	0.6279	0.6028	0.5026	98JA	0.0031	0.1002
	SO	0.7667	0.702	0.9043	0.8762	98SO	0.0647	0.0281

EVAPORATION RATES (inches/day)								
	Mar	Apr	May	Jun	Jul	Aug	Sep	Oct
Ak1N	0.17	0.27	0.30	0.38	0.43	0.37	0.30	0.20
Ak4E	0.17	0.27	0.30	0.38	0.43	0.37	0.30	0.20
CPER	0.17	0.24	0.28	0.29	0.33	0.27	0.20	0.14
FC	0.04	0.15	0.18	0.21	0.23	0.21	0.16	0.10
FM	0.17	0.24	0.28	0.29	0.33	0.27	0.20	0.14
Wray	0.17	0.24	0.29	0.37	0.4	0.35	0.27	0.19

Table 4.2: Average daily evaporation rates for the sites under study in inches. (Note: Ak1N uses Ak4E rates. FM and CPER use Wiggins rates. Wray uses a Bonny Dam/Ak4E average. All but FC use John Martin Dam rate for March because of similarity of their evaporation profiles and the missing March rates at these sites.)

far exceeded the estimated daily evaporation rate for that month for that site (see Table 4.2) had the following day's data removed as well. This was to reduce the possibility that the degree of latent heat flux partitioning would be caused by the evaporation of standing water or excessively moist soil from the previous rain event instead of from the vegetation itself.

4.5 Time Frame

The time frame utilized for the data sets was March through October in the years 1989 to 1998. March is considered early or pre-spring and in some instances greening begins in this month. October was considered the end of summer and was included for completeness and comparative analysis. Further, regreening sometimes occurs in the natural landscape after the late summer senescent phase passes.

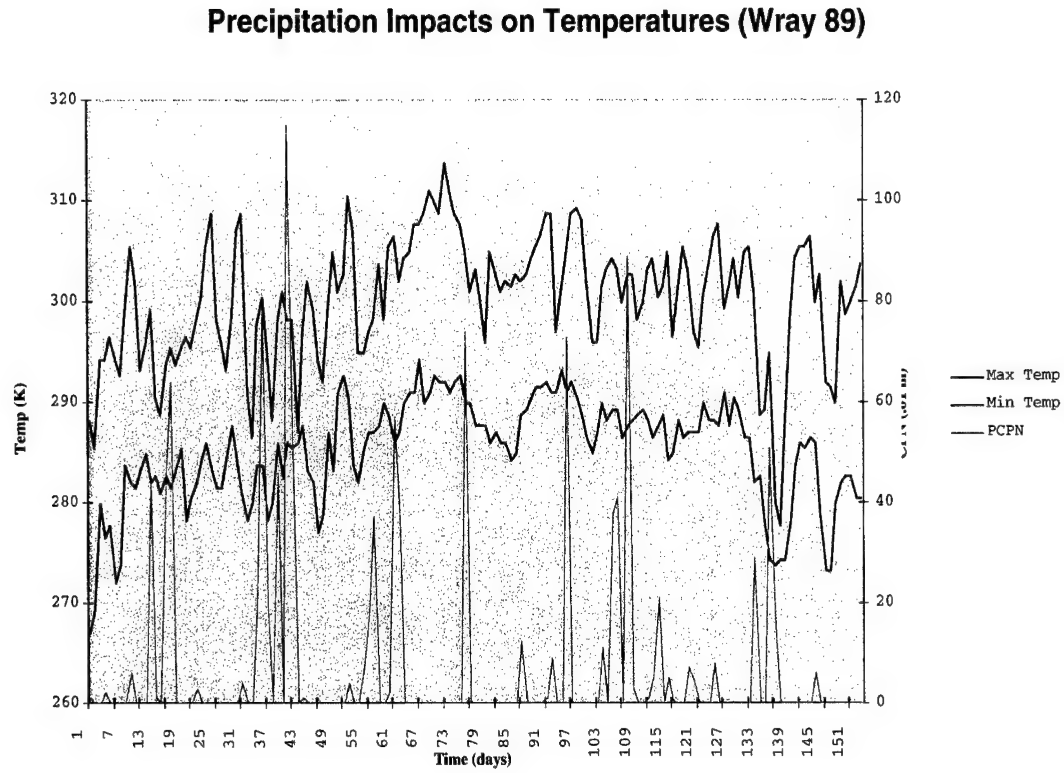

Figure 4.1: Precipitation impacts on temperatures (Wray 89), shows how surface temperatures change in response to precipitation events. The Wray 89 depiction is representative of all sites and all years studied.

4.6 Analyses

First, the robust LTS regressions were performed for the time period extending from the March to October time frame excluding the precipitation event days, for each site for each year 1989 through 1998. Second, the regressions were then performed over the same time periods broken into four two-month blocks of March-April, May-June, July-August, and September-October, to evaluate if a seasonal pattern was discernible. An analysis of statistical significance was then performed. All values that fell below the 95 percent confidence level ($p>0.5$) were deleted from the analysis. Then the remaining $r-$squared values for the 850-700 mb layer mean and surface temperature analyses were

subtracted from the $r-$squared values of the 850-700 mb layer mean with NDVI and surface temperature analyses (regressions without vegetation) for the temperature maxima and minima. This produced an $r-$squared difference value. Finally, at each site the four time-block $r-$squared difference values were each time-averaged over the years under study. For example, all the March-April Wray maximum temperature $r-$squared difference values were averaged over 1989-1998. This averaged $r-$squared difference value was then graphed and compared to the other time-block values for Wray and the other sites. The data deletions due to lack of statistical significance greatly impacted the CPER maximum temperature $r-$squared values, leaving only one value (i.e., one year's averaged values – 1995, a period of slow transition between a moderate El Niño and a weak La Niña event) to be averaged over the July-August time block and three values (three years – 1989, a strong La Niña year, and 1992 and 1998, which had strong El Niño events) averaged for the March-April time blocks. This is in contrast to the 7 to 10 years of data that were averaged for the other sites. The minimum temperature $r-$squared values at CPER were not affected significantly. Figures 5.1–5.2 for the maxima and 5.3–5.4 for the minima show the difference that the 95 percent significance level had as compared to the raw data (no significance assessed).

Chapter 5

RESULTS

5.1 $r-$squared Comparisons

As described in Section 4.6, the final analysis performed was that of time-block averaged $r-$squared difference values for 1989 through 1998 at the 95 percent confidence level. Figure 5.1 and 5.3 display the results of these averaged $r-$squared difference values. For comparison, Figs. 5.2 and 5.4 depict maximum and minimum $r-$squared difference values for all data regardless of statistical significance. The disparity between the different sites is immediately noticeable. However, of significant note is that all the averaged $r-$squared difference values for all sites for both the maximum and minimum temperatures were positive. This implies that there is a consistent and significant improvement in explanation of surface temperature maxima and minima by including the vegetational influences via the NDVI values. There were negative (see Appendix B) individual $r-$squared difference values for 28 out of 414 measurements, giving a 6.8 percent occurrence rate. However, of the 28 negative $r-$squared difference values not one was greater than 0.0023. No values explained more than 0.23 percent of the surface temperature variance. Figure 5.5 shows the comparison of magnitudes between one of the largest negative $r-$squared difference values (0.0022) and the rest of the values from that site. Clearly the negative values lacked significant impact (Fig. 5.5). On the other hand, 42 values were positive $r-$squared difference but were less than 0.5 percent and were likewise of negligible impact. This left 344 $r-$squared difference values that were positive and explained more than 0.5 percent of the variance in the surface temperature. These 344 values ranged from 0.5 to an extreme of 52.24 percent. These greater $r-$squared difference values coincide with the greater averaged $r-$squared difference values in Figs. 5.1 and 5.3. The $r-$squared difference values

depict the difference in the explanation of the variance of the surface temperature maxima and minima because of the inclusion of vegetation influences. The averaged $r-$squared difference values ranged from 1.6 to 20.8 percent. Averaging these values produced a mean maximum surface temperature explained value of 5.6 percent, and a mean minimum surface temperature explained value of 8.5 percent. These explained values are increases over the degree of explanation using the 850-700 mb layer mean temperature alone.

These increases were in spite of mitigating impacts and factors from some of the sites and sensor locations. These mitigating influences are examined in Appendix C.

5.2 Diurnal Variations

Distinct diurnal variations are seen by comparing Figs. 5.1 and 5.3. The magnitudes of the variations are driven by each site's microclimatic conditions. With one exception, vegetation had a greater impact on the minimum temperature than on the maximum temperature at every site. Type 3 sites had the greatest average differences, averaging 7.6 percent for Fort Morgan and 6.8 percent for Wray. Wray also held the greatest average diurnal extremes of 1.9 and 11.9 percent. On the other end of the spectrum, the Type 2 sites had the least average differences, averaging 0.2 and 0.4 percent for Akron 1N and Akron 4E, respectively. Akron 4E also had the smallest extremes of average diurnal difference values, ranging from 0.4 to 1.2 percent. Fort Collins, the Type 4 site, had an average diurnal difference of 2.8 percent, falling between the Type 2 and 3 site averages. CPER, the exception noted above, had an average diurnal difference of 0.4 percent greater explanation of the maximum temperatures over the minimum temperatures.

5.3 Seasonal Variations

Clear seasonal variations are also displayed in Figs. 5.1 and 5.3. These variations have many causes, most of which are site specific. Possible explanations for these variations are examined in Appendix C.

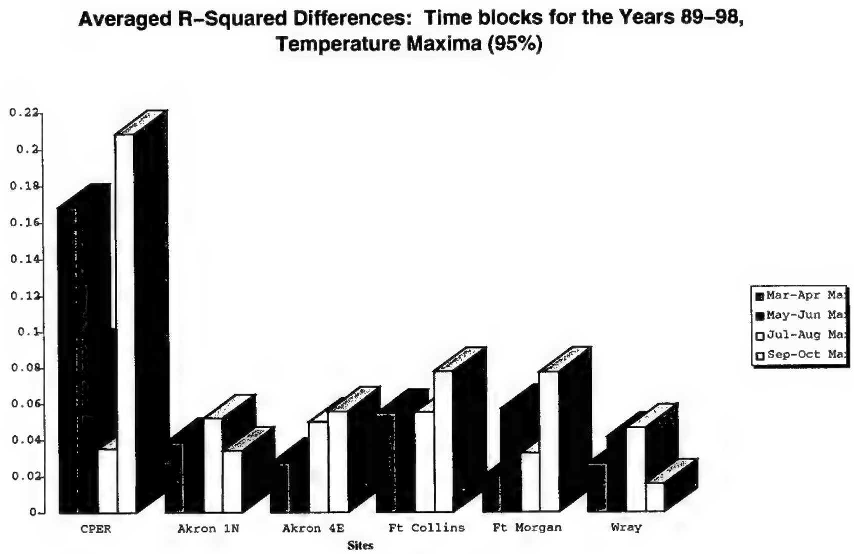

Figure 5.1: Averaged $r-$squared differences. Time blocks for the years 1989-1998. Maximum temperatures. Shows the $r-$squared difference between the 850-700 mb layer mean temperature maxima correlated to the surface temperature maxima subtracted from the same layer mean temperature extrema including vegetation impacts via NDVI values correlated to the surface temperature extrema. Values are significant to 95 percent confidence level.

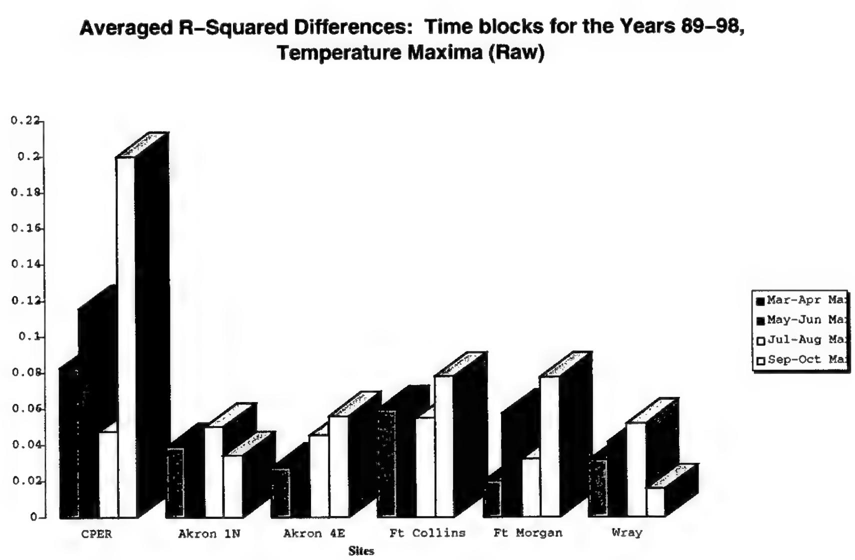

Figure 5.2: Same as Fig. 5.1 except all data was included prior to significance-test deletions for comparison.

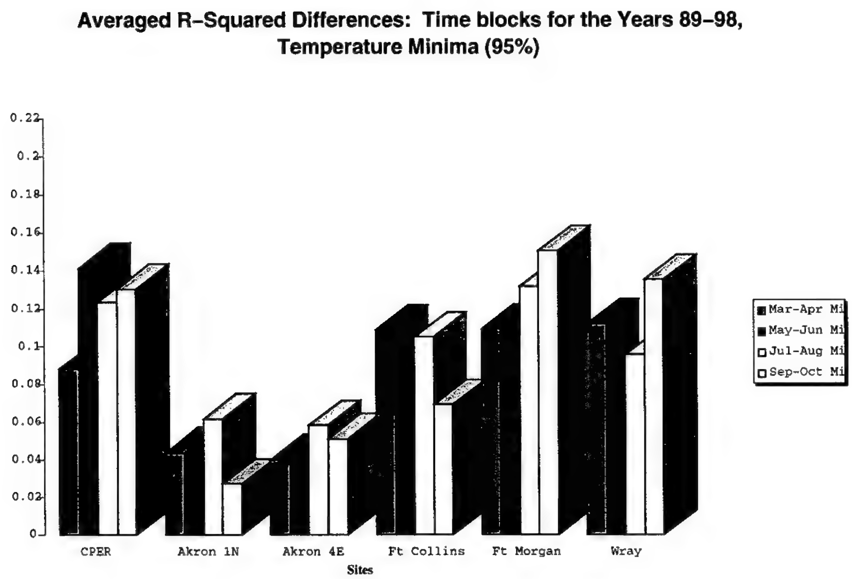

Figure 5.3: Same as Fig. 5.1 except for minimum temperatures. Values are significant to 95 percent confidence level.

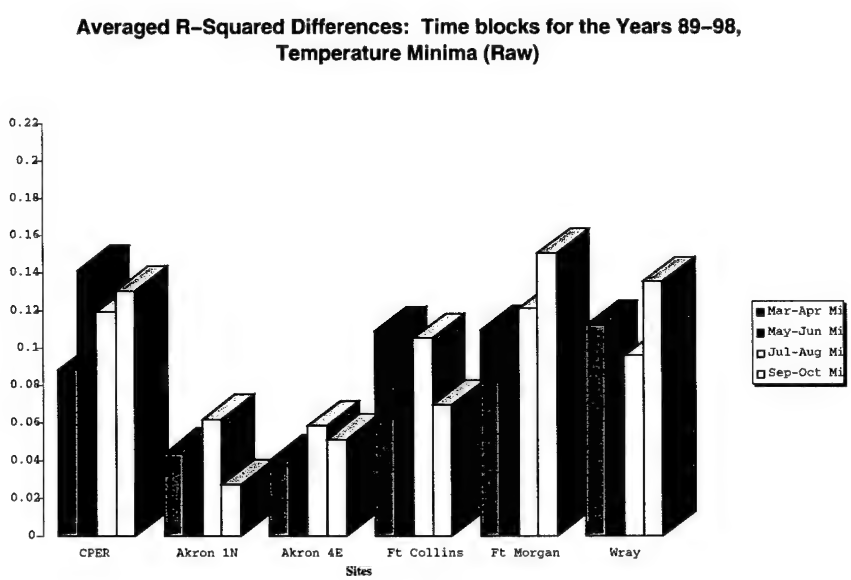

Figure 5.4: Same as Fig. 5.3 except all data was included prior to significance-test deletions for comparison.

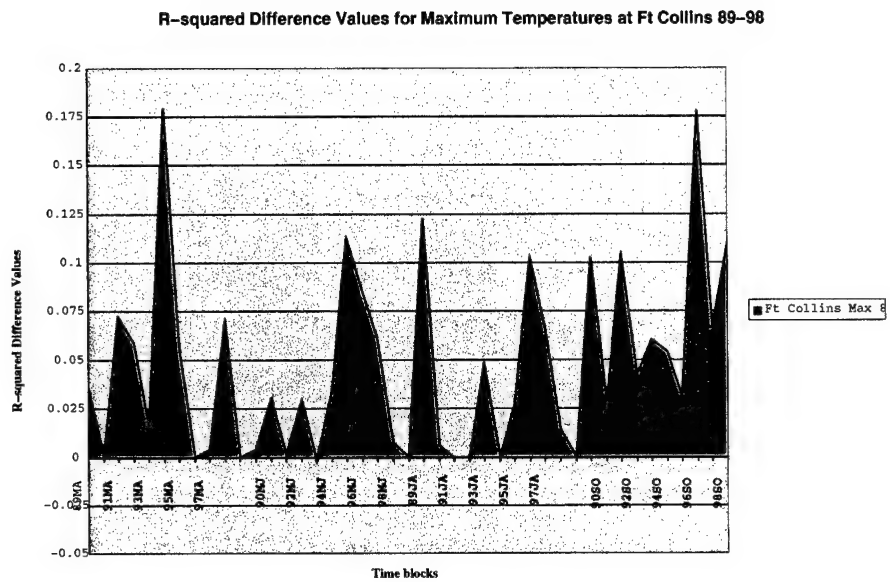

Figure 5.5: $r-$squared difference values for maximum temperatures at Fort Collins for 1989-1998. The negative $r-$squared value of 0.0022 (one of the largest in this analysis) appears where the 93MJ mark would be. The difficulty in seeing the displayed value underscores its lack of impact to the analysis compared to the rest of the displayed values.

5.4 Interannual Variation

There were no specific trends seen concerning interannual variability.

5.5 Site Ranking

Thematic grouping, or ranking, according to site characteristics was detailed in the site designations section of Chapter 2 and further for each site in Section 2.3. To recap, of the five graduations considered, only four were utilized for this work. The spectrum ran from CPER, a pristine Type 1 site to Fort Collins, a rural-urban Type 4 site. The site maximum and minimum $r-$squared difference values were averaged across each Type to give values indicative of the characteristics of that class. CPER, the most natural site with the least anthropogenic influences, had the greatest overall increase in explained variance for both day and night compared to the other Type-averaged categories. [On a site-to-site comparison, Fort Morgan, a Type 3 site, had a slightly greater increase in explained variance for minimum temperatures (12.3 percent) over CPER (12.1 percent).] However, Fort Collins, the most urban and anthropogenically-influenced site, had a slightly greater maximum temperature average $r-$squared difference value than the Type 2 or Type 3 sites. The minimum temperature explained variance increase at Fort Collins was greater than the Type 2 sites but less than that of the Type 3 sites. The Type 2 and 3 sites had similar maximum temperature $r-$squared difference profiles. The corresponding minimum temperature profiles, however, show a marked difference between the two anthropogenic-influenced sensor sites and the two that had less anthropogenic influences.

The greatest average vegetational influences are seen in the Type 1 environment, with an average $r-$squared increase of 12.5 percent for the maximum temperatures and 12.1 percent for the minimum temperatures. This Type 1 site was the only class where the average $r-$squared difference increase for the maximum temperatures was greater than that for the minimum temperatures. The least overall changes in surface temperature due to vegetational influences is in the pristine-rural, Type 2, areas, showing an average of 3.7 percent increase for maxima and 4.0 for minima. This may be a result of extra latent

heat fluxes from soil moistened by irrigation. Compared to Type 2, Type 3 sites have a nearly equal average daytime vegetational impact, increasing by an average of 3.9 percent. Comparatively, they have an increased nighttime influence from vegetation, averaging just below 11.2 percent. This could occur as a result of the anthropogenic influences losing their impact on the sensible heat flux component in the close proximity of the sensor when the sun goes down. Type 4 average $r-$squared increases were 5.6 percent for maxima and 8.4 percent for minima. Table 5.1 summarized these results.

Table 5.1: Shows site category (type), designation, short description of site characteristics, example of this type used in this work, and the average increased r−squared value for the maximum and minimum temperatures, respectively.

TYPE	DESIGNATION	DESCRIPTION	EXAMPLE	AVERAGE INCREASED r−SQUARED VALUE (MAX/MIN)
1	Pristine	Very little to no anthropogenic influences	CPER	12.5/12.1
2	Pristine-Rural	Some anthropogenic influences though widely surrounded by pristine-class landscape	Akron 1N, Akron 4E	3.7/4.0
3	Rural	Strongly influenced by anthropogenic factors though widely surrounded by pristine to pristine-rural landscape	Fort Morgan, Wray	3.9/11.2
4	Rural-Urban	Receives strong vegetational influences though widely surrounded by urban character landscape	Fort Collins	5.6/8.4
5	Urban	Almost no vegetational influences, completely dominated by urban character	None in this work	

Chapter 6

CONCLUSIONS

The primary thrust of this work has been to show that there is definite and positive value added by the inclusion of vegetation parameters in the analysis of the surface temperatures.

Among the conclusions, sensor location and placement are concerns and need to be addressed by the National Weather Service. The example of Fort Morgan, with its sensor 3 m from a north-shielding brick factory building, and 2.5 m from the exhaust of a window air conditioner, can only give temperature readings that are representative of that very isolated area. Wray is in a similar situation. The question of representativeness must be determined and appropriate placement action taken to avoid the skewing of temperature data. This especially true of sites that are routinely used for climate studies.

This work has clearly shown that there is a greater degree of explanation for the surface temperatures from the combination of 850-700 mb layer mean temperatures and NDVI values than for the 850-700 mb layer mean temperatures alone. Further, the results indicate that with the exception of CPER, the minimum temperatures on average, are explained more by the inclusion of the NDVI data in the analysis than for the maximum temperatures for all other sites and for all years. The seasonal variations are quite pronounced and vary from site to site and can be explained in part by the location and the influences of the specific vegetation around each site.

As a result of these site-specific conditions, five categories were created to account for and better analyze the variations that occurred between the sites. The most pristine site, with the least amount of anthropogenic influences, was found to have the greatest average increase in explained variance for both maximum and minimum surface temperatures.

The inclusion of NDVI data in the analysis increases the percentage of explained variance for the maximum temperatures between 1.6 percent and 20.8 percent, with an average of 6 percent, and the minimum temperatures between 1.7 percent and 15.1 percent, with an average of 8 percent.

This would indicate that the inclusion of NDVI data could increase the predictability of maximum and minimum temperatures. Further study should be conducted at other sites to confirm these results. Future work should utilize a significantly larger sample size of sites that encompass or represent all five site categories. Parameterizations of the sensible and latent heat fluxes can be made after specific experiments and analyses over all categories of sites are thoroughly examined. The ultimate goal is to derive a technique that adequately and accurately considers and ingests the vegetational impacts in the analysis of the surface temperature extrema.

6.1 Future Work

Considering a larger number of sites over a larger spatial area (i.e., the Midwest or the Great Plains) would ensure a larger database from which to work. The University of Oklahoma Mesonet could be a useful resource to this end. An area more densely populated with surface observation sites that include radiosonde launch locations could more accurately reveal correlating relationships. Including a greater number of pristine-class sites could help establish, with a greater degree of certainty, a more definitive baseline for the degree of vegetation impacts. Further, including a sample of locations that satisfy the full range of site categories could give a more robust view of the total impact of vegetation on the surface temperature extrema.

A dedicated field campaign, or incorporation into another field campaign, would be useful. Sensible and latent heat fluxes could be measured directly by use of eddy covariance methods or approximated using bulk aerodynamic formulae. This data, along with the basic parameters of temperature, precipitation, evaporation, and vegetation type, could be ingested with other parameters, including ground flux measurements, wind speed and

direction, and cloud days and types, to give a numerical result to the surface energy balance equation.

As MODIS (Moderate Resolution Imaging Spectroradiometer) products become more available, utilizing its higher spatial resolution (250 m) and tighter spectral bands could bring a greater degree of confidence and accuracy to the vegetation greenness measurements.

Determining a regional vegetational impact coefficient would be useful for ingesting in forecast analyses, numerical models, and climate studies. The ultimate goal is to derive a model scheme that adequately and accurately considers and ingests the vegetational impacts in the analysis, and ultimately, the surface temperature extrema.

REFERENCES

Arya, S., 1988: *Introduction to micrometeorology.*, Academic Press, San Diego, 307 pp.

Avissar, R., 1996: Potential effects of vegetation on the urban thermal environment. *Atmos. Env.*, **30**, 437-448.

Charney J.G., W.J. Quirk, S.H. Chow, and J. Komfield, 1977: A comparative study of the effects of albedo change on drought in semi-arid regions. *J. Atmos. Sci.,* **34**, 1366-1385.

Chase, T.N., 1999: The role of historical land-cover changes as a mechanism for global and regional climate change. Ph.D. Dissertation, Atmospheric Science Paper No. 685, Colorado State University, R.A. Pielke, P.I., 117 pp.

Clements, F., 1916: *Plant succession.* Carnegie Institute, Washington, 512 pp.

Cowan, I., 1968: Mass, heat and momentum exchange between stands of plants and their atmospheric environment. *Quart. J. Roy. Meteor. Soc.*, **94**, 523-544.

Dirmeyer, P.A., and J. Shukla, 1996: The effect on regional and global climate of expansion of the world's deserts. *Quart. J Roy. Meteor. Soc.*, **122**, 451-482.

Farnsworth, R., and E. Thompson, 1982: Mean monthly, seasonal, and annual pan evaporation for the United States. NOAA Technical Report NWS 34, 23-25.

Fitzjarrald, D., O. Acevedo, and K. Moore, 2001: Climate consequences of leaf presence in the eastern United States. *J. Climate*, **14**, 598-614.

Henderson-Sellers, A. and V. Gornitz, 1984: Possible climatic impacts of land cover transformations with particular emphasis on tropical deforestation. *Climatic Change*, **6**, 231-257.

Holdridge, L.R., 1947: Determination of world plant formations from simple climatic data. *Science*, **105**, 367-368.

Meehl, G.A., 1994: Coupled land-ocean-atmosphere processes and south Asian monsoon variability. *Science*, **266**, 263-267.

Monteith, J., 1975: *Vegetation and the atmosphere.* Volume 1, Academic Press, San Francisco, CA, 278 pp.

Panofsky, H, and G. Brier, 1968: *Some applications of statistics to meteorology.* The Pennsylvania State University, University Park, PA, 224 pp.

Philip, J., 1964: Sources and transfer processes in the air layers occupied by vegetation. *J. Appl. Meteor.*, **3**, 390-395.

Pielke, R.A., R.L. Walko, L. Steyaert, P.L. Vidale, G.E. Liston, and W.A. Lyons, 1999: The influence of anthropogenic landscape changes on weather in south Florida. *Mon. Wea. Rev.*, **127**, 1663-1673.

Pielke, R.A., T. Stohlgren, W. Parton, J. Moeny, N. Doesken, L. Schell, and K. Redmond, 2000: Spatial representativeness of temperature measurements from a single site. *Bull. Amer. Meteor. Soc.*, **81**, 826-830.

Pielke, R.A., T. Stohlgren, L. Schell, W. Parton, N. Doesken, K. Redmond, J. Moeny, T. McKee, and T.G.F. Kittel, 2001: Problems in evaluating regional and local trends in temperature: An example from eastern Colorado, USA. *Int. J. Climatol.*, submitted.

Potter, G.L., H.W. Ellsaesser, M.C. MacCracken, and J.S. Ellis, 1981: Albedo change by man. *Nature*, **291**, 47-49.

Raschke, K., 1956a: Mikrometeorologisch gemessene energieumsätze eines alocasiablattes. *Arch. Meteor. Geophys. Bioklimatol.*, **7**, 240-268.

Raschke, K., 1956b: Uber die physikalischen beziehungen zwischen warmeuberganszahl strahlungsaustausch, temperatur und transpiration eines plattes. *Planta*, **48**, 200-238.

S-PLUS 4 Guide to Statistics, Data Analysis Products Division, MathSoft, Seattle, WA, 146-147.

Sagan, C., O.B. Toon, and J.B. Pollack, 1979: Anthropogenic climate changes and the earth's climate. *Science*, **206**, 1363-1368.

Schwartz, M., 1994: Monitoring global change with phenology: The case of the spring green wave. *Int. J. Biometeorol.*, **38**, 18-22.

Segal, M., R. Avissar, M.C. McCumber, and R.A. Pielke, 1988: Evaluation of vegetation effects on the generation and modification of mesoscale circulations. *J. Atmos. Sci.*, **45**, 2268-2292.

Segal, M., W. Schreiber, G. Kallos, R.A. Pielke, J.R. Garratt, J. Weaver, A. Rodi, and J. Wilson, 1989: The impact of crop areas in northeast Colorado on midsummer mesoscale thermal circulations. *Mon. Wea. Rev.*, **117**, 809-825.

APPENDIX A: NLCD LAND COVER CLASSIFICATION SYSTEM DEFINITIONS

The following tables show the 1 km and 5 km data for each site for the following National Land Cover Data Classes.

21-Class National Land Cover Data Key:

Water

11 Open Water

12 Perennial Ice/Snow

Developed

21 Low Intensity Residential

22 High Intensity Residential

23 Commercial/Industrial/Transportation

Barren

31 Bare Rock/Sand/Clay

32 Quarries/Strip Mines/Gravel Pits

33 Transitional

Forested Upland

41 Deciduous Forest

42 Evergreen Forest

43 Mixed Forest

Shrubland

51 Shrubland

Non-natural Woody

61 Orchards/Vineyards/Other

Herbaceous Upland

71 Grasslands/Herbaceous

Herbaceous Planted/Cultivated

81 Pasture/Hay

82 Row Crops

83 Small Grains

84 Fallow

85 Urban/Recreational Grasses

Wetlands

91 Woody Wetlands

92 Emergent Herbaceous Wetlands

Table A.1: Akron 1N 1 and 5 km data.

Land Cover Class	1 km Number of Pixels	1 km Percent	5 km Number of Pixels	5 km Percent
Class 11	0	0	59	0.07
Class 12	0	0	0	0
Class 21	475	13.95	933	1.1
Class 22	0	0	0	0
Class 23	256	7.52	1691	1.99
Class 31	0	0	194	0.23
Class 32	0	0	0	0
Class 33	0	0	0	0
Class 41	0	0	0	0
Class 42	0	0	2	0
Class 43	0	0	0	0
Class 51	0	0	0	0
Class 61	0	0	0	0
Class 71	1990	58.44	58235	62.56
Class 81	2	0.06	287	0.34
Class 82	51	1.5	1643	1.93
Class 83	383	11.25	13224	15.54
Class 84	248	7.28	13822	16.24
Class 85	0	0	0	0
Class 91	0	0	0	0
Class 92	0	0	0	0

Table A.2: Akron 4E 1 and 5 km data.

Land Cover Class	1 km		5 km	
	Number of Pixels	Percent	Number of Pixels	Percent
Class 11	0	0	24	0.03
Class 12	0	0	0	0
Class 21	0	0	134	0.16
Class 22	0	0	0	0
Class 23	168	4.94	1253	1.47
Class 31	0	0	160	0.19
Class 32	0	0	0	0
Class 33	0	0	0	0
Class 41	0	0	0	0
Class 42	0	0	2	0
Class 43	0	0	0	0
Class 51	0	0	0	0
Class 61	0	0	0	0
Class 71	2712	79.22	39776	46.75
Class 81	0	0	119	0.14
Class 82	0	0	825	0.97
Class 83	136	4	15616	18.36
Class 84	386	11.35	27169	31.93
Class 85	0	0	0	0
Class 91	0	0	0	0
Class 92	0	0	0	0

Table A.3: CPER 1 and 5 km data.

Land Cover Class	1 km		5 km	
	Number of Pixels	Percent	Number of Pixels	Percent
Class 11	0	0	59	0.07
Class 12	0	0	0	0
Class 21	0	0	0	0
Class 22	0	0	0	0
Class 23	0	0	1121	1.32
Class 31	0	0	34	0.04
Class 32	0	0	0	0
Class 33	0	0	0	0
Class 41	0	0	0	0
Class 42	0	0	2	0
Class 43	0	0	0	0
Class 51	0	0	706	0.83
Class 61	0	0	0	0
Class 71	3401	100	73122	86.07
Class 81	0	0	66	0.08
Class 82	0	0	0	0
Class 83	0	0	5219	6.14
Class 84	0	0	4625	5.44
Class 85	0	0	0	0
Class 91	0	0	0	0
Class 92	0	0	0	0

Table A.4: Fort Collins 1 and 5 km data.

Land Cover Class	1 km Number of Pixels	1 km Percent	5 km Number of Pixels	5 km Percent
Class 11	6	0.18	4063	4.78
Class 12	0	0	0	0
Class 21	2194	64.4	34107	40.14
Class 22	580	17.02	4966	5.84
Class 23	240	7.04	3955	4.65
Class 31	0	0	411	0.48
Class 32	0	0	0	0
Class 33	0	0	0	0
Class 41	0	0	242	0.28
Class 42	0	0	2	0
Class 43	0	0	0	0
Class 51	0	0	100	0.12
Class 61	0	0	0	0
Class 71	29	0.85	6194	7.29
Class 81	11	0.32	6797	8
Class 82	5	0.15	6795	8
Class 83	3	0.09	29	0.03
Class 84	63	1.85	1185	1.39
Class 85	276	8.1	16119	18.97
Class 91	0	0	0	0
Class 92	0	0	0	0

Table A.5: Fort Morgan 1 and 5 km data.

Land Cover Class	1 km Number of Pixels	1 km Percent	5 km Number of Pixels	5 km Percent
Class 11	352	10.38	2568	3.02
Class 12	0	0	0	0
Class 21	338	9.96	6256	7.36
Class 22	0	0	574	0.68
Class 23	106	3.13	1056	1.24
Class 31	0	0	36	0.04
Class 32	0	0	0	0
Class 33	0	0	0	0
Class 41	0	0	0	0
Class 42	0	0	0	0
Class 43	0	0	0	0
Class 51	0	0	0	0
Class 61	0	0	0	0
Class 71	1410	41.57	32749	38.52
Class 81	320	9.43	9877	11.62
Class 82	522	15.39	26100	30.7
Class 83	27	0.8	91	0.11
Class 84	245	7.22	4644	5.46
Class 85	12	0.35	872	1.03
Class 91	57	1.68	159	0.19
Class 92	3	0.09	31	0.04

Table A.6: Wray 1 and 5 km data.

Land Cover Class	1 km Number of Pixels	1 km Percent	5 km Number of Pixels	5 km Percent
Class 11	0	0	78	0.09
Class 12	0	0	0	0
Class 21	0	0	966	1.14
Class 22	0	0	30	0.04
Class 23	29	0.85	637	0.75
Class 31	1	0.03	215	0.25
Class 32	0	0	0	0
Class 33	0	0	0	0
Class 41	0	0	47	0.06
Class 42	1	0.03	155	0.18
Class 43	0	0	0	0
Class 51	0	0	0	0
Class 61	0	0	0	0
Class 71	3257	95.91	61993	72.86
Class 81	92	2.71	728	0.86
Class 82	16	0.47	12000	14.1
Class 83	0	0	7984	9.38
Class 84	0	0	9	0.01
Class 85	0	0	248	0.29
Class 91	0	0	0	0
Class 92	0	0	0	0

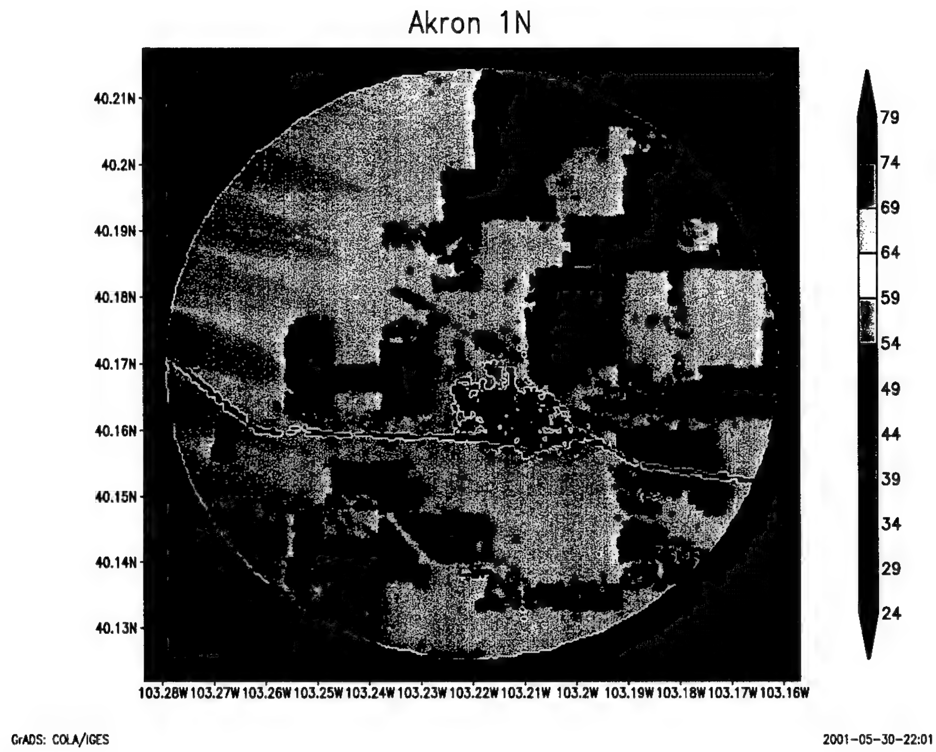

Figure A.1: 5 km radius circle of 30 m resolution land-use data for Akron 1N.

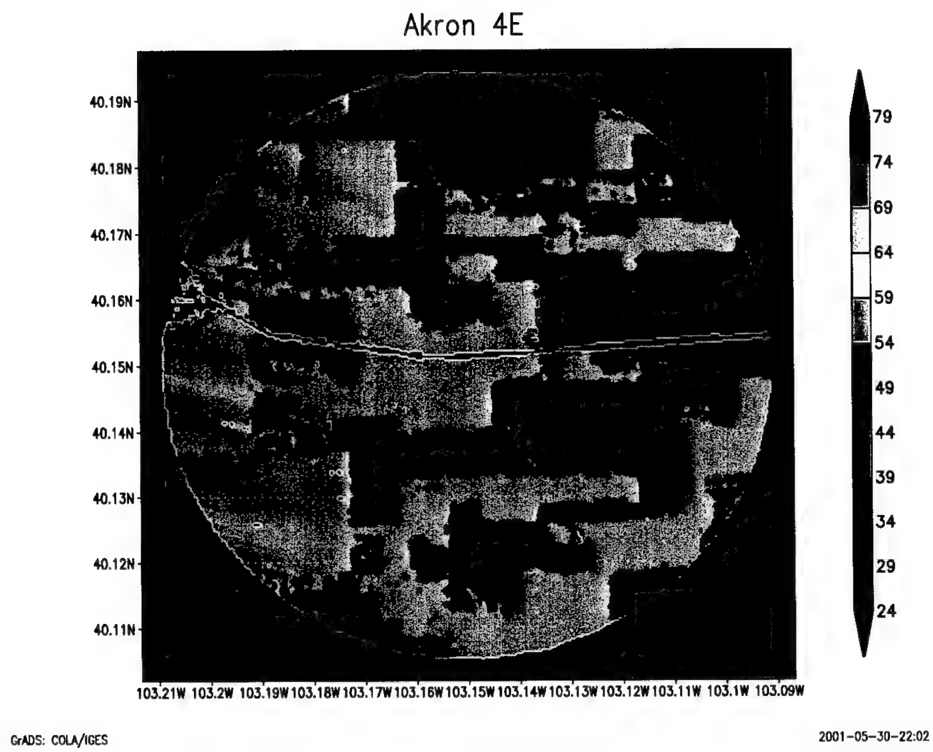

Figure A.2: 5 km radius circle of 30 m resolution land-use data for Akron 4E.

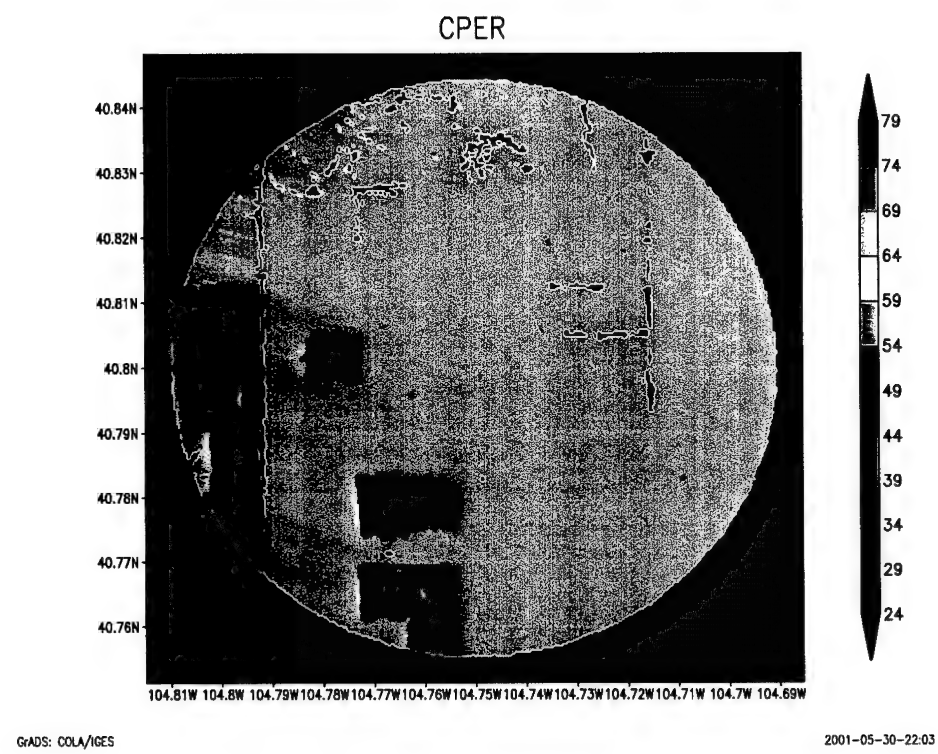

Figure A.3: 5 km radius circle of 30 m resolution land-use data for CPER.

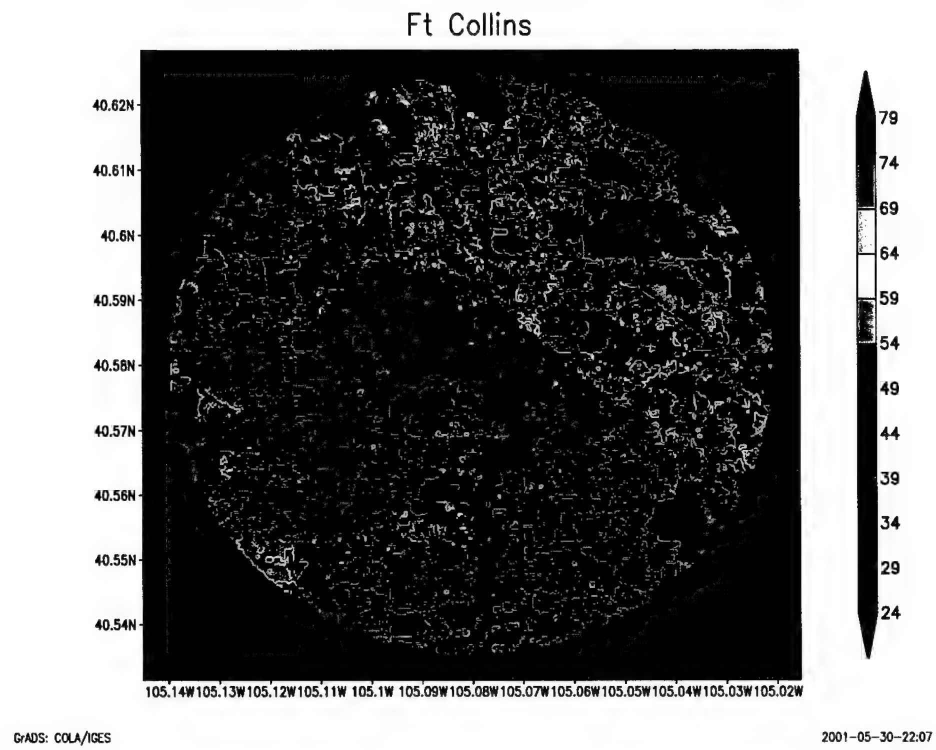

Figure A.4: 5 km radius circle of 30 m resolution land-use data for Fort Collins.

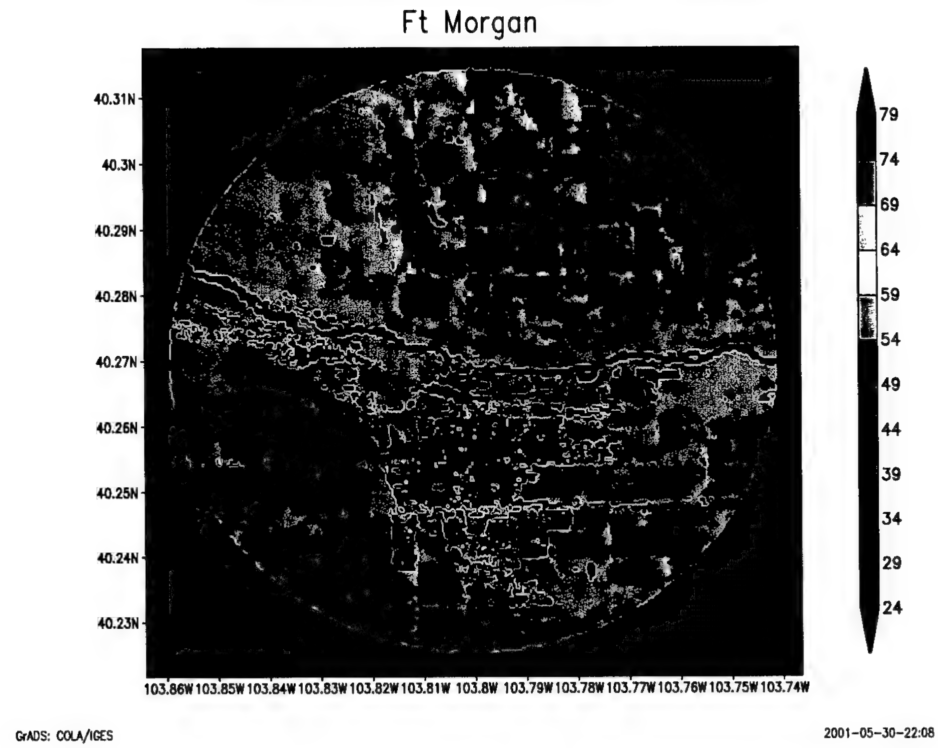

Figure A.5: 5 km radius circle of 30 m resolution land-use data for Fort Morgan.

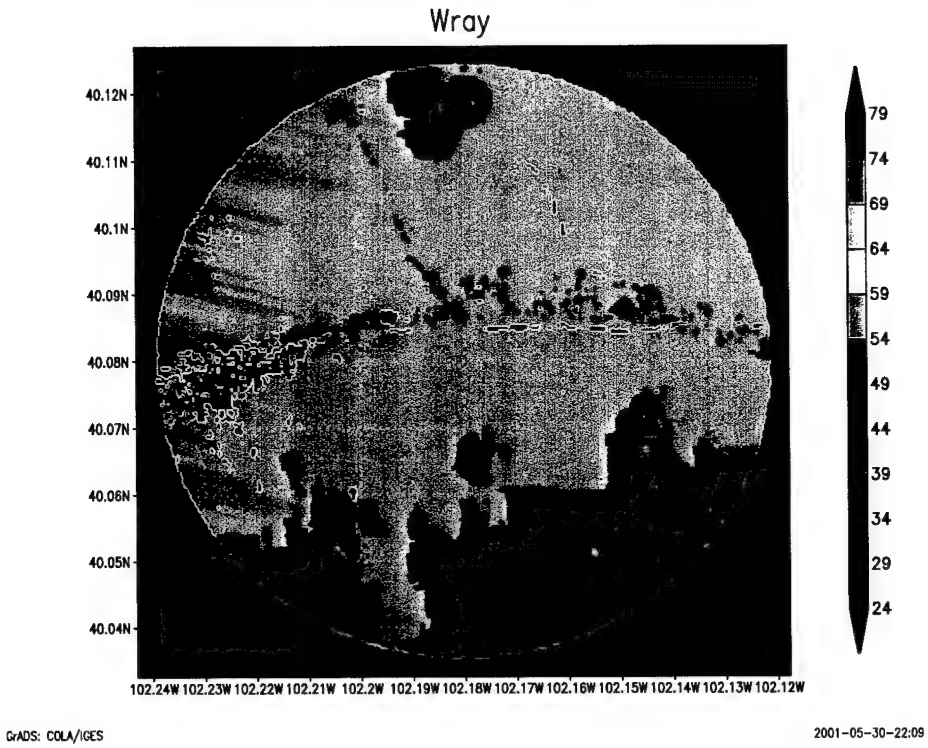

Figure A.6: 5 km radius circle of 30 m resolution land-use data for Wray.

APPENDIX B: SHORT COURSE IN STATISTICS

The following statistical concepts were utilized for this work.

B.1 Variance

The variance is the average of the square of the deviation of a measure from its mean

$$\left[\sum (x - x_m)^2\right] / n - 1,$$

where the summation is from $i = 1$ to $i = n$ and the subscript m denotes the mean of that measurement.

B.2 Covariance

The covariance of two variables measures their tendency to vary together, i.e., to co-vary. The covariance is the average of the products of the deviations of measures from their means

$$\sum \left[(x_i - x_m)(y_i - y_m)\right] / n - 1,$$

where the summation is from $i = 1$ to $i = n$ and the subscript m denotes the mean of that measurement. The degree of "co-varying" is important, but when comparing data from different data sets it is useless to discuss the covariance on its own merit due to the possible or probable incompatibilities between the scales of measure (units and magnitude) of the data. The covariance is useful (in the context of this work) only when normalized to contend with the differing scales of measurement (Mielke 2001, personal communication). The covariance is normalized by the product of the standard deviations

of the two variables. A normalized covariance is given the designation of r.

$$r = \sum xy / \left[\left(\sum x^2\right)\left(\sum y^2\right)\right]^{0.5},$$

where $x = x_i - x_m$ and $y = y_i - y_m$. A normalized covariance is one definition of a correlation, and the r-value is the coefficient of linear correlation.

B.3 Correlation

Correlation is the strength of the association between two variables or data sets. The coefficient of linear correlation (or simply correlation coefficient), r, holds values between -1 and $+1$. An r-value close to $+1$ means there is a strong positive correlation, and both data variables tend to increase or decrease together. An $r-$value near -1 means there is a strong negative correlation, and as one variable tends to increase, the other decreases. If the $r-$value is zero, then there is no relationship at all between the two variables. To summarize, the $r-$value is very useful in determining positive and negative association as well as the degree of association between two data sets or sets of measurement values. Panofsky and Brier (1968) describe the correlation coefficient as the square root of the ratio of explained to total variance of a variable, and having the sign of the slope of the lines of regression.

Stated another way, the correlation coefficient can be defined as the square root of the coefficient of determination.

B.4 Coefficient of Determination

Perhaps even more useful (especially for this work) than the degree of correlation is the $r-$squared value, the coefficient of determination.

$$r^2 = \sum (xy)^2 / \left[\left(\sum x^2\right)\left(\sum y^2\right)\right]$$

Sometimes referred to incorrectly as the explained variance, the coefficient of determination is more accurately the ratio of the explained variance over the total variance between

the two sets of measurement values. Stated another way, $r-$squared describes the proportion of variance in common between the two variables. Multiplying $r-$squared by 100 gives the percent variance in common between the two variables, or the percentage of variation in one variable that is explained by the variation in the second variable. This percent tells how much of the predicted or dependent variable is explained by the predictor or independent variable. $r-$squared values can tell how much predictability in percent a certain measurement can give toward the resultant value of another measurement. $r-$squared values from multiple predictor variables can have a synergistic effect on explaining the predicted variable. If the predictor variables are independent of each other, the $r-$squared values are simply additive. If the predictor variables are not independent, the $r-$squared values are not additive but do contain significant information. If by adding a second or third predictor the $r-$squared value increases, the explanation or predictability of the predicted variable is increased. For example, let's say (hypothetically) the number of red cars sold per year to men has an $r-$squared value of 0.78 and the number of cars that also have a tow bar package added per year sold to men has an $r-$squared value of 0.83 (i.e., 83 percent of all cars that have tow bar packages added were sold to men – not a big surprise there). Although the relationship between the number of red cars sold and the number of cars that have tow bar packages installed that are sold are not independent of each other, the $r-$squared value from the three variables can clearly show an increase or decrease in the relationship and the resultant prediction. If the $r-$squared value of the number of red cars sold with tow bar packages installed to men is 0.94, then a clear increase in explanation and predictability is shown. Ninety-four percent of the red cars with tow packages installed will be sold to men. Taking this into account with the estimated number of male buyers will better enable the dealerships to predict the number of tow packages required for a given number of red cars. This, of course, is a simplified and hypothetical case.

B.5 Negative r^2 Difference Values

Negative r^2 difference values are possible when the "independent" variables are not truly independent. Thus the correlation between the two "independent" variables may exceed the correlation between the "independent" variables and the dependent variable. The equation (Panofsky and Brier 1968)

$$R^2_{3.21} = \frac{r^2_{31} + r^2_{32} - 2r_{31}r_{32}r_{12}}{1 - r^2_{12}}$$

shows that it is possible to have a multiple correlation coefficient that is less than a single correlation coefficient. The subscripts 1, 2, and 3 indicate the 1st, 2nd, and 3rd variables and r is the coefficient correlation between the two subscripted variables. For example, let the variables 1 and 2 be the "independent" variables that in reality have a correlation. Variable 3 is the dependent variable. If the correlation between the independent variables (r_{12}) is greater than that between the 2nd and 3rd variables, there is a possibility for a reduced R^2 compared to the value without variable 2. It can be shown that

$$\frac{r_{31}}{r_{32}} + \frac{r_{32}}{r_{31}} < \frac{r_{12}}{2} \text{ or } \frac{r^2_{31} + r^2_{32}}{r_{32}r_{31}} < \frac{r_{12}}{2}$$

will produce a reduced R^2 (or r^2 in this work) that will result in a negative r^2 difference value. In this case variable 1 in the 850-700 mb layer mean temperature extrema, variable 2 is the NDVI value, and variable 3 is the surface temperature extrema.

APPENDIX C: QUALITATIVE INTERPRETATIONS

C.1 General

During the day, the planetary boundary layer (PBL) tends to be well-mixed, sweeping or mixing away much of the detectable change in the Bowen ratio due to the influence of the vegetation. The decoupling of the PBL at night suppresses this vertical mixing, leaving more of the vegetational impacts on temperatures to be seen in the analysis. This can be seen in the general trend of diurnal temperature responses to vegetational impacts.

The climatological character of precipitation changes through the time frame under study and impacts the vegetation greenness. In April to early June synoptic systems provide the bulk of the precipitation via widespread and steady rainfall along with some convective storms. This time frame is also a period of increased greening. From late June through September, drier conditions exist as the predominant precipitation events come from isolate convective storms. Browning of the vegetation occurs in non-irrigated areas in response to vegetational stress and senescence.

C.2 Site Layout/Sensor Location Impacts

C.2.1 Akron 1N

Maximum Temperatures

The maximum temperatures show a drop in vegetational influence from the first to second time blocks, and then a sharp increase during the third. The September-October

time frame sees another drop nearly equal in magnitude to the drop in the second time block. The small grain belts, fallow areas, and pasture lands that surround the site increase in greenness during the initial time block and transpire commensurately. The second time block experienced temperatures which increased more rapidly than the small-leafed grains could moderate. This drop in the vegetational influence is seen in the concurrent drop in the analysis during that time block. The third time block saw an increase in the vegetational influence upon the maximum temperatures. This increase could be explained by the pastures grasses attaining their full growth and that vegetation reaching maturity during this time frame. The fourth time block would indicate a time of reduced greenness, which occurs in the early fall. The temperatures drop more quickly than the change in greenness, although the greenness changes still influence the maximum temperatures. The relatively low average vegetational influence of about 3.5 percent may be caused by the aircraft apron and runway to the immediate west and by the metal structures to the north and south of the sensor. Since the predominant wind flow generally comes from the west these mitigating influences would be expected to impact the temperature scheme and reduce the detectable vegetational impacts. See Fig. 5.1.

Minimum temperatures

The minimum temperatures, like the majority of the sites experienced a drop in the vegetational impact in the second time block (May-June). This could be because the vegetation is greening up during this time, but the temperatures are increasing more dramatically than the vegetation is able to modify the temperatures. The pasture land vegetation and small grain crops would be growing and greening but would lack the leaf area of mature crops. This lack of leaf area would create a commensurate lack of influence. By the late summer (July-August) the crops are mature and should have a more robust influence, which is reflected in the increased r−squared difference value for the third time block. As with the maximum temperatures, significant mitigating effects may have occurred from the nearby concrete aircraft apron and runway to the immediate west of

the sensor during the intervening time of beginning green up and when the vegetation is mature and its influence is greatest. The concrete would radiate its heat rather quickly after the cessation of the radiation input (sundown). It would continue to radiate longwave radiation and cool its surface much more than the surrounding vegetationally-influenced landscape. This impact can be seen in the relatively low average $r-$squared difference value and specifically in the second and fourth time blocks. In the early fall the temperatures begin to fall more quickly than the drop off of the greenness of the landscape. The pasture vegetation continues to impact the locale but the lush green of the landscape begins to be edged with brown, due to dead or senescent stomatal areas, and the ability to transpire is reduced. Since the transpired moisture near the vegetation surface is reduced, the nocturnal latent heat partitioning agent, condensation on radiatively cooled vegetation, is commensurately reduced. These impacts are seen in the reduction of the vegetational influence. The area is predominately influenced by the short grasses of the pastures surrounding the site. See Fig. 5.2.

C.2.2 Akron 4E

Maximum Temperatures

The first two time blocks show a trend that is moderated but similar to Akron 1N, as the pasture land grasses green up and grow. The increase in impact in the third time block would correspond to the time of grasses attaining full maturity and would be expected as the large areas of transpirational agents are at their peak. The fourth time block would be indicative of a period of regreening and the recovery from any late summer senescent periods or impacts. It is theorized that the irrigated nature of the fields immediately surrounding the site acts as an anthropogenic influence for most of the time periods, altering the Bowen ratio, and reducing the average $r-$squared difference value. The fourth time block in particular shows strong resurgence in the vegetational impact.

This is likely due to the irrigated state of the crops allowing them to remain green longer. See Fig. 5.1.

Minimum Temperatures

The minimum temperature $r-$squared difference values generally follow the pattern of Akron 1N, and for many of the same reasons, for the first three time blocks. Although there is no large stretch of concrete (other than the highway nearby) to dramatically modify the temperature scheme, the irrigated condition of the crops could be moderating the vegetational influence as well as enhancing the regreening in the fourth time block. By providing a source of latent heat flux that alters the Bowen ration, this impact could mask some of the vegetational influences. See Fig. 5.2.

C.2.3 CPER

Maximum Temperatures

CPER experienced the highest maximum temperature impacts from vegetation of the sites studied. The immediate vicinity of the site is short grass pasture. The initial greening of the vegetation shows its influence in the first time block. Since there is no irrigation in the near proximity of the site, the heat of summer initiates the onset of senescence and is reflected in a progressive and dramatic drop in the second and third time block. The area has limited leaf area coverage, exposing nearly 50% bare soil. Combined with the predominantly senescent state of late summer, the small vegetational impact is not unexpected. The fourth time block shows the impact of the strong annual regreening period of that landscape and its resultant increased vegetational influence. See Fig. 5.1.

Minimum Temperatures

As the grasses green and mature, their impacts can be seen to increase. Even during the daytime senescence of late summer, the evening still saw much latent heat partitioning via condensation on the radiationally cooled the leaf surface. This impact was reduced slightly in the third time block. Since the vegetation experiences a period of regreening, the latent heat partitioning is increased through increased radiational cooling and condensation. The impact from the vegetation is thus increased during the fourth time block. See Fig. 5.2.

C.2.4 Fort Collins

Maximum Temperatures

By virtue of being a city, Fort Collins has a unique signature over the time blocks. The initial greenness impact of the first time block drops and then slowly increases throughout the summer. This may be explained by the many watered lawns in the surrounding area. Further, Fort Collins has a significantly larger number and greater density of trees than any of the other sites examined. Mitigating the greenness impacts are the influences of the many streets and structures that comprise the city. The vegetational influences seem to overcome the tendency toward the heat island effect that a city can experience.

Minimum Temperatures

Minimum temperature impacts closely follow the trend of Akron 1N, though roughly double in magnitude. The trees and highly irrigated lawns that Akron 1N lacks may explain the magnitude differences. The aircraft apron and metal buildings in such close proximity of Akron 1N may give a close simulation of urban impacts, resulting in similar seasonal trends with the strongly urban-impacted Fort Collins site.

C.2.5 Fort Morgan

Maximum Temperatures

The Fort Morgan vegetational influence trends run nearly opposite to every other site examined. The increase in the first two time blocks shows the greening and impact of the pastures and row crops. The third period shows a drop in impact, most probably due to late summer senescence. The regreening of fall, and its increased impact, is seen in the September-October time frame. The local landscape should exert a much greater degree of influence but does not due to the placement of the sensor. The south-facing brick building radiates heat on sunny days. Likewise, the window air conditioner exhaust that blows across the sensor must impact the temperature reading the skew the vegetational influences. Still, the landscape impacts are present, though not of the magnitude one would expect of the surrounding area. The greatest mitigating factor for this site is the brick, concrete and steel factory that completely blocks all northerly influences, including that of the Platte River just to the north of the site.

Minimum Temperatures

After dropping from the first time block, the vegetational impacts increase through the remaining three periods. Some of the highest average $r-$squared difference values are found at this site in September-October. This may be due to the residual warming of the sensor from the factory structure being masked as vegetational influence. The resultant values are not unexpected, considering the landscape surrounding the Fort Morgan area. Considering the site location, though, implies that the values are probably not dominated by the true vegetational impacts.

C.2.6 Wray

Maximum Temperatures

The influence on the maximum temperature increases from the first to third time block, then drops markedly in the fourth. A possible explanation, similar to the situation in Fort Morgan, is that the radio station building where the sensor is installed is having a strong influence on the maximum temperatures and thus to some degree mitigates the vegetational influences.

Minimum Temperatures

Showing an opposite trend from the maximum temperature plot, there is a dramatic drop between the first and second time blocks then a steady and equally dramatic increase throughout the rest of the periods. Again, as with Fort Morgan, a possible explanation may be that the proximity of the building to the sensor and the radiation given off by the building at night may mask the temperature profiles as having stronger vegetational impact. Considering the surrounding landscape, the values are not unexpected. Though the values imply a strong vegetational impact, as with Fort Morgan, other influences may be mitigating them from purely landscape influences.